Novel Materials and Modeling Techniques for Energy Conversion and Storage Devices

by Kulbhushan Vashisth

B.E. in Electrical Engineering, May 2008, Deenbandhu Chhotu Ram University of Science and Technology, Haryana, India

A Thesis submitted to

The Faculty of
School of Engineering and Applied Science
of The George Washington University
in partial fulfillment of the requirements
for the degree of Masters of Science

May 19, 2013

Thesis directed by

Robert J. Harrington
Professor of Engineering and Applied Science

Dedication

The author wishes to thank all family members for their support.

Acknowledgements

I deeply acknowledge my thesis advisor, Professor Robert J. Harrington, who provided me the guidance and encouragement to pursue this thesis work. This work would not have been possible without his support and feedback. I learned a great deal about reading research papers, and choosing research topics after taking multiple courses taught by him. He is a role model and truly a scholar. I also thank him for recruiting me for the masters program in electrical engineering in the focus area of power and energy. I highly recommend this program for future students. I am very thankful to Prof. Nedal Deeb for serving on my thesis committee, guiding me on many industry-relevant aspects, and teaching me much about power system reliability and related topics that I extensively studied in excellent courses taught by him. My fellow graduate students and departmental staff members deserve thanks for their camaraderie as they greatly contributed to my graduate experience at GWU.

I am forever indebted to my parents, my brother, and other family members for their unwavering support in every manner possible. I am highly grateful to them for encouraging me to pursue a degree in higher education.

Abstract

"Novel Materials and Modeling Techniques for Energy Conversion and Storage Devices"

This thesis describes the functioning of some of the state-of-the art energy conversion and storage devices. The working mechanisms, underlying parts, and novel materials required for construction of these devices are also discussed. This is followed by a focus on the modeling and simulation techniques for supercapacitors and photovoltaic cells as specific cases. In the end, outlook and conclusions on the materials and modeling techniques in use for energy conversion and storage devices is presented, and some ongoing challenges in achieving a wide-spread usage of such devices are also briefly discussed.

Table of Contents

Dedication ii

Acknowledgments iii

Abstract of Thesis iv

List of Figures vi

List of Tables viii

Chapter 1: Introduction 1

Chapter 2: Energy conversion and storage devices 3

Chapter 3: Novel materials for energy conversion and storage devices 16

Chapter 4: Modeling techniques for supercapacitors 26

Chapter 5: Modeling techniques for photovoltaic cells 46

Chapter 6: Outlook and conclusions 53

References 56

Appendices 59

List of Figures

Figure 1……4

Figure 2……6

Figure 3……7

Figure 4……8

Figure 5……..10

Figure 6……....11

Figure 7……...…11

Figure 8……...……13

Figure 9……...……14

Figure 10……..15

Figure 11……..19

Figure 12……..22

Figure 13……..23

Figure 14……..24

Figure 15……..25

Figure 16……..27

Figure 17……..28

Figure 18……..29

Figure 19……..31

Figure 20……..33

Figure 21……..34

Figure 22……..35

Figure 23……..37

Figure 24……..38

Figure 25……..39

Figure 26……..42

Figure 27……..43

Figure 28……..44

Figure 29……..46

Figure 30……..48

Figure 31……..49

Figure 32……..50

Figure 33……..51

Figure 34……..51

Figure 35……..52

List of Tables

Table 1……18

Chapter 1: Introduction

1.1 Energy conversion and storage

Due to changing global landscape, energy has become a major focus of research in the scientific community primarily driven by an increased demand around the world. A significant interest in this direction has been to develop and refine more efficient and advanced energy conversion and storage devices. Therefore, it is essential to design highly-efficient, low-cost, and safe materials for applications in various energy conversion technologies and devices in response to the energy needs of modern society and ever-increasing environmental as well as ecological concerns. Not only one needs novel materials for efficiency in these devices, but also new modeling and simulation techniques are needed to test a variety of parameters that can affect the performance characteristics of a specific device. These factors are furthermore coupled with the economics and energy balance over the life time of a device. The purpose of this work is to provide a comprehensive and critical overview and assessment of the state-of-the-art materials as well as modeling and simulation techniques for selected energy conversion and storage devices. In the following, the contents of this thesis are briefly described.

1.2 Thesis outline

The outline of this thesis is as follows.

Chapter 2 introduces in brief the various types of selected energy conversion and storage devices, their functioning, and related mechanisms.

Chapter 3 highlights key novel nanomaterials that are in use for specific energy conversion and storage devices, the advantages and disadvantages of such materials, and discussion on possibilities for improvements.

Chapter 4 describes the modeling and simulation techniques for supercapacitors as emerging energy storage systems. This chapter also highlights key software used for implementing these modeling and simulation methods.

Chapter 5 details the modeling and simulation techniques for photovoltaic cells that are used to better estimate the sensitivity of performance characteristics to various parameters.

Chapter 6 provides a brief outlook on the materials and modeling techniques in use for energy conversion and storage devices, and also discusses some ongoing challenges in achieving a wide-spread usage of such devices.

Some key references for the entire work are listed in the end.

Chapter 2: Energy conversion and storage devices

2.1 Introduction

There are many different types of devices that are available for energy conversion and storage usage. The major energy conversion and storage devices include electrochemical capacitors, photovoltaic cells, lithium batteries, fuel cells, and physics-based energy conversion devices, etc. In this chapter, the working principles of some of these devices relevant to this work will be outlined, and their functioning and mechanisms will be discussed.

2.2 Performance comparisons of various devices

The performance comparison of various energy storing devices is done by plotting a type of chart known as the Ragone plot. On such a chart, the values of energy density are plotted against power density both on logarithmic axes, and this representation allows comparison of the performance of different devices in terms of high and low power. The vertical axis describes the amount of available energy, while horizontal axis represents the rate at which energy is delivered. The plot in Figure 1 shows and compares the power density against the energy density for the most important energy storage systems today. As illustrated in this plot, supercapacitors occupy a key position in terms of the specific energy and the specific power because they have a significantly lower energy density in comparison to batteries but they also have a higher power density in comparison to batteries. The area for batteries is very common to standard lithium-ion batteries, but there are some key difference in the manner in which these devices work. The principles

of batteries is to use chemical processes to store energy via separation of charge, while supercapacitors use electrolytic dielectrics to achieve very high capacitance compared to conventional capacitors and thereby can attain greater energy densities.

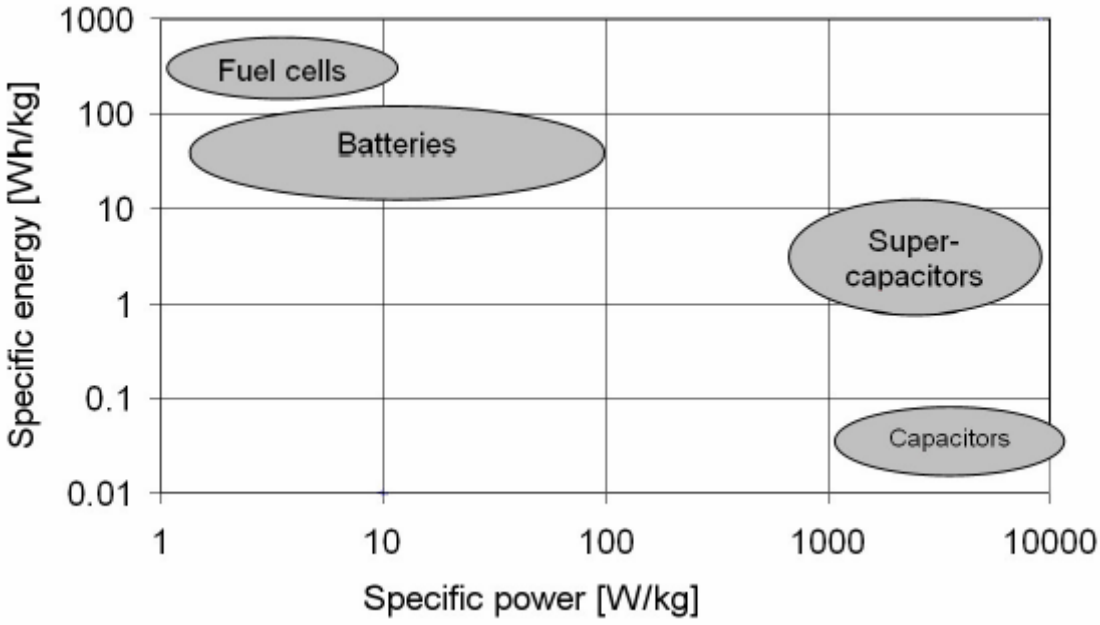

Figure 1: Specific power against specific energy, also called a Ragone plot, for various electrical energy storage devices.

In the following, the functioning, types, and mechanisms of a few selected devices are discussed.

2.3 Definition: Supercapacitors

Supercapacitors, also known as the electrochemical capacitors or ultra-capacitors, are devices that can store and deliver energy at relatively high rates (beyond those accessible with batteries) because the mechanism of energy storage is the simple charge-separation at the electrochemical interface between the electrode and the electrolyte.

Supercapacitors are of key importance in supporting the voltage of a system during increased loads in everything from portable equipment to electric vehicles. These devices occupy the area in the Ragone plot (Figure 1) between batteries and dielectric capacitors. Supercapacitors are similar to batteries in design and manufacture (two electrodes, separator, and electrolyte), but are designed for long cycle life and high power.

Conventional capacitors have two conducting electrodes separated by an insulating dielectric material. Opposite charges accumulate on the surfaces of each electrode when a voltage is applied to a capacitor. The dielectric works as a charge separation medium, thereby creating an electric field and storage of energy in the capacitor, as illustrated in Figure 2.

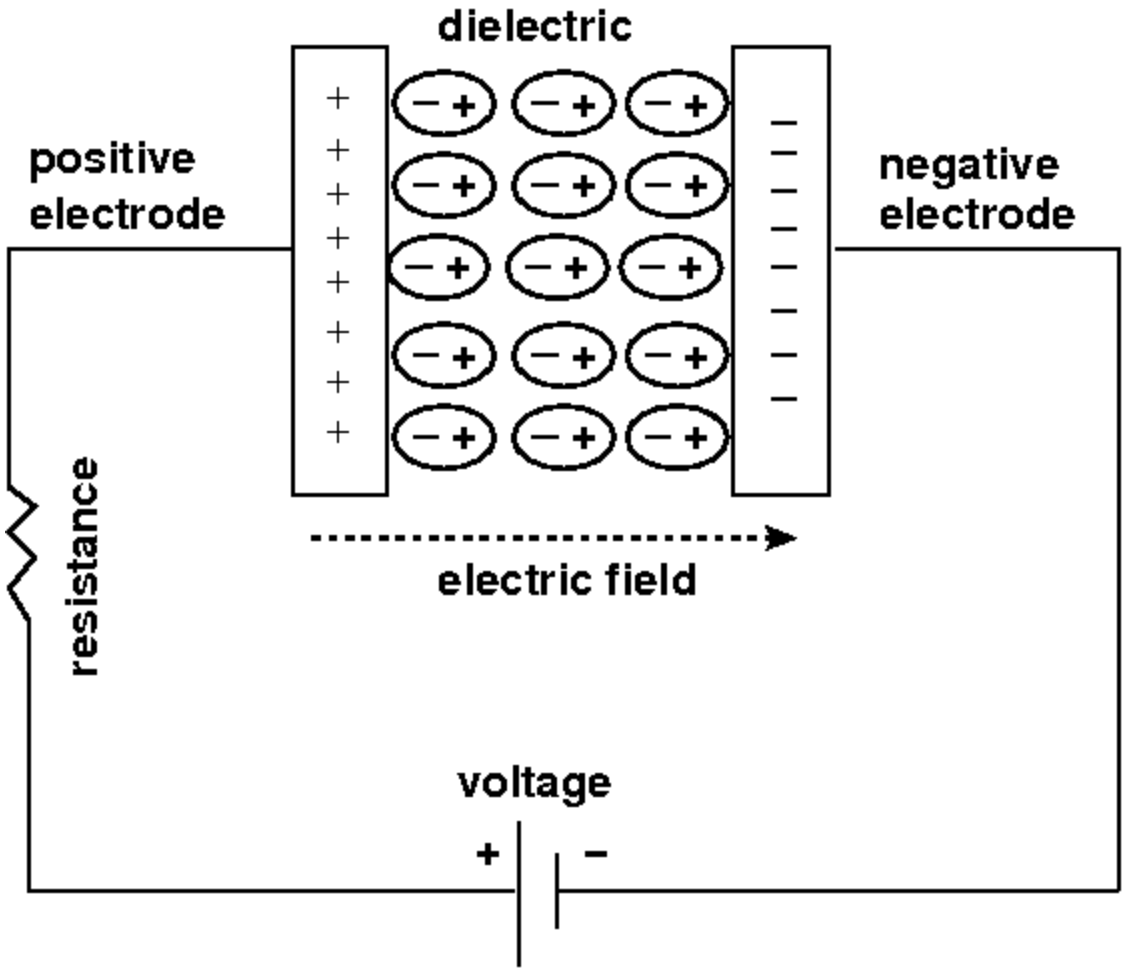

Figure 2: Schematic of a conventional capacitor.

Although the power densities of conventional capacitors are high, their energy densities are significantly lower than electrochemical batteries and fuel cells as pointed out above. In other words, the energy stored in capacitors can be discharged rapidly but total storage capacity is less. Therefore, supercapacitors were designed on same principles as conventional capacitors to have electrodes with higher surface areas and thinner dielectrics, which lead to increased energy storage. Supercapacitors also have shorter charging times, and longer shelf-life in comparison to batteries. A general schematic of a supercapacitor is provided in Figure 3.

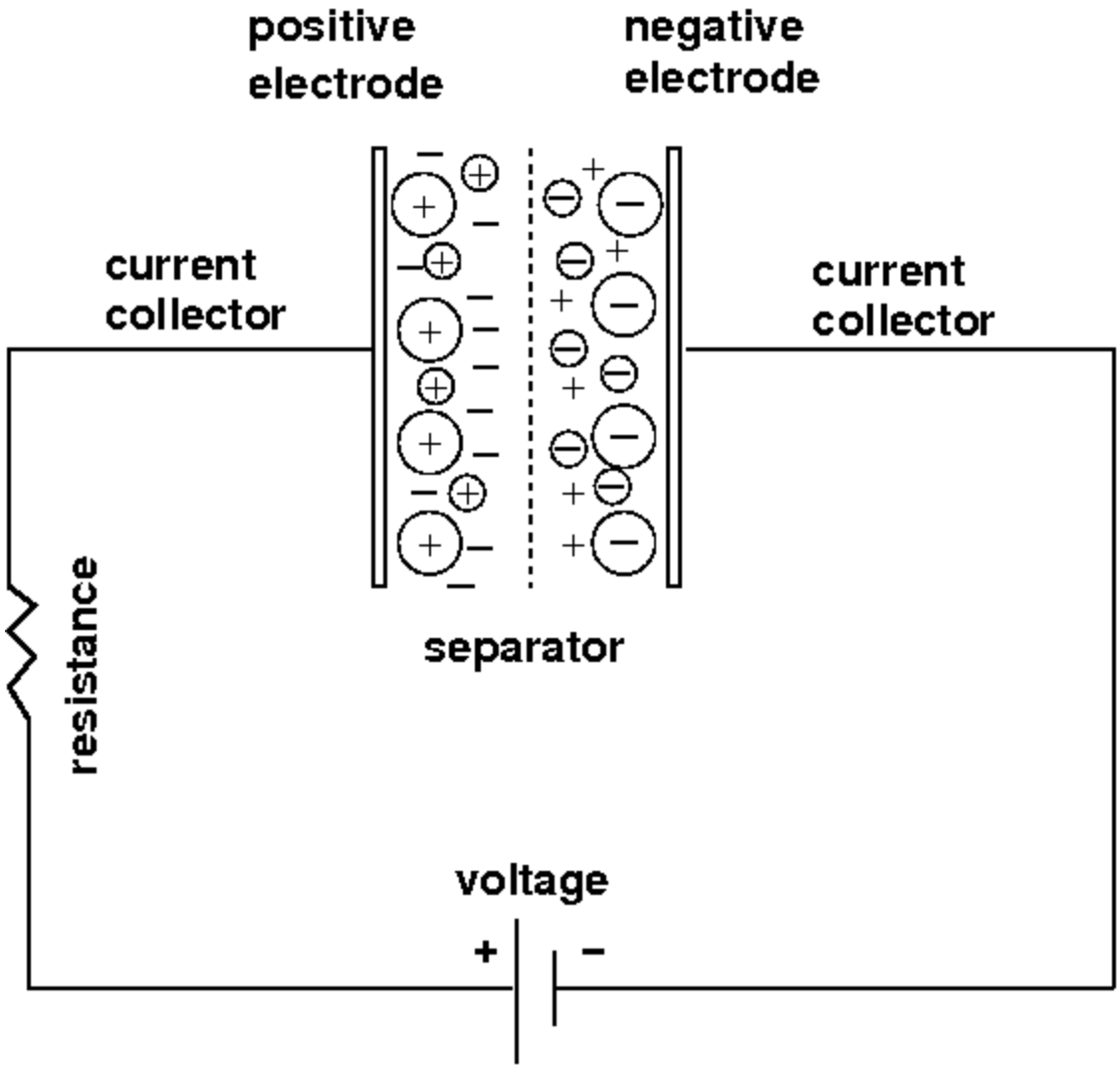

Figure 3: Schematic of an electrochemical supercapacitor.

2.3.1 Classification

Several types of ECs can be distinguished, depending on the charge storage mechanism as well as the materials used. However, there are primarily two general categories of electrochemical capacitors:

(a) Electric Double Layer Capacitors (EDLC)

(b) Redox supercapacitors

In contrast to batteries, where cycle life is limited because of repeated contraction and expansion of electrode on cycling, EDLC lifetime is in principle infinite because it operates solely on electrostatic charge accumulation. In the case of redox supercapacitors, some fast charge transfer takes place as in a battery giving rise to large pseudo-capacitance. The schematic of a commercial EDLC is shown in Figure 4.

Figure 4: (a) Schematic of a commercial spirally wound double layer capacitor. (b) Assembled device weighing 500 g. (c) A small button cell [1].

2.3.2 Principles of energy storage in supercapacitors

General mechanisms: The way that supercapacitors store energy is based on two types of capacitive behavior. The first is electrical double layer (EDL) capacitance from pure electrostatic charge accumulation at the electrode interface, and the second is pseudo-capacitance developed from fast and reversible surface redox processes at characteristics

potentials.

EDLC Mechanism: EDLCs store the charge electrostatically using reversible adsorption of ions of the electrolyte onto active materials that are electrochemically stable and have high specific surface area (SSA). Charge separation occurs at the electrode-electrolyte interface, producing what Helmholtz first described in 1853 as the double layer capacitance *C*. Capacitance *C* is defined as the ratio of stored charge *Q* to the voltage applied *V*:

$$C = \frac{Q}{V} . \quad (1)$$

For conventional capacitors, the capacitance C is also given by:

$$C = \epsilon_0 \varepsilon_r \frac{A}{d}. \quad (2)$$

where *A* is the electrode surface area, *d* is effective thickness of double layer, and rest of the terms are dielectric constants of electrolyte and vacuum. The charge storage in EDLCs is highly reversible resulting in high cycling stabilities (10^6 cycles). In comparison, batteries may only last for 10^3 cycles. For these reasons, EDLCs are better suited for applications where once does not need to provide user-based service such as mountains or deep sea applications.

There are various models for supercapacitors. The double layer model of Helmholtz is similar to that of two-plate conventional capacitors. The simple model of Helmholtz was modified by Gouy and Chapman on consideration of a continuous distribution of ions in electrolyte solution, driven by thermal motion, which is called as the diffuse layer. Later,

Stern combined the Helmholtz model with the Gouy-Chapman model to explicitly recognize two regions of ions distribution-the inner region called as the compact or Stern layer, and the diffuse layer. These three models are summarized in Figure 5.

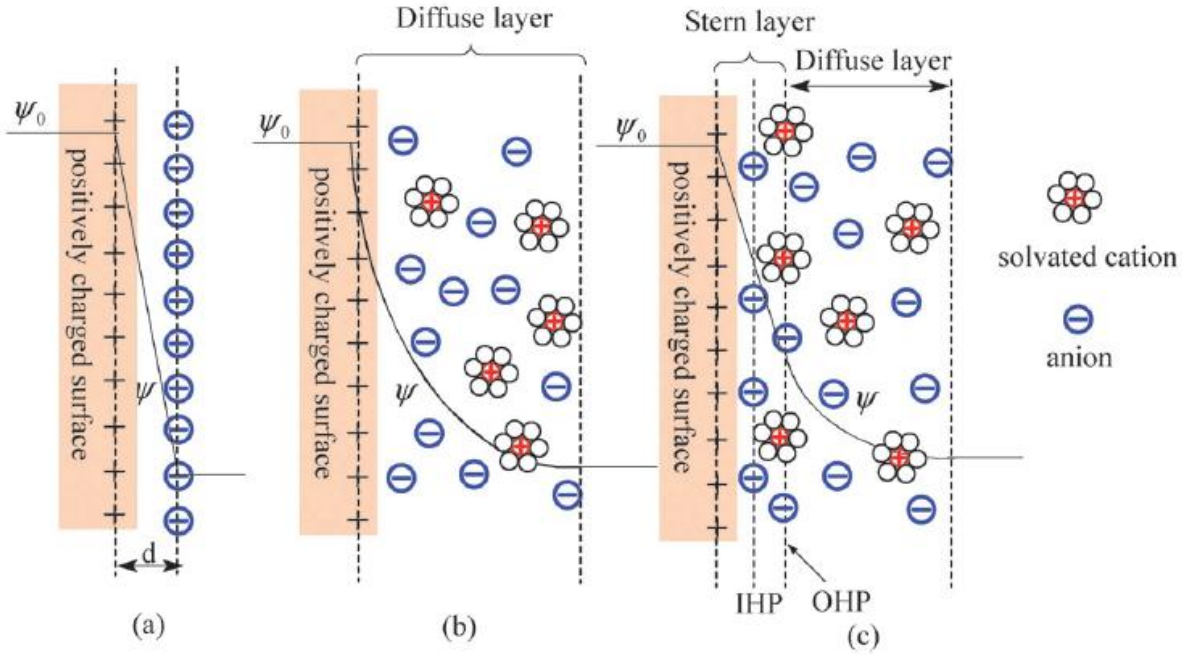

Figure 5: (a) Helmholtz model. (b) Guoy-Chapman model. (c) Stern model. IHP and OHP are inner and outer Helmholtz planes [2].

The capacitance in the EDL can be treated as a combination of the Stern type of double layer capacitance and the diffusion region capacitance. The factors that determine EDL behavior at a planar electrode surface include the electrical field across the electrode, the types of electrolyte ions, the solvent in which ions are dissolved, and the chemical affinity between ions and the electrode surface. The behavior of a typical EDLC laboratory cell is shown in Figure 6, whose rectangular voltammogram is characteristic of a pure double layer capacitance mechanism.

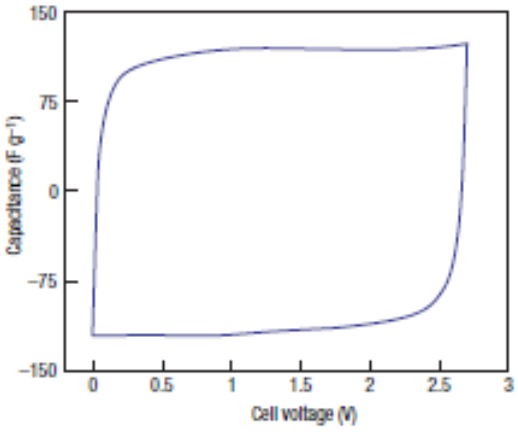

Figure 6: Cyclic voltammogram of a two electrode laboratory EDLC cell [1].

The electrode is usually a porous material with a high SSA. An EC electrode must be considered as a blocking electrode from an electrochemical point of view. Initial research was devoted to increasing pore volume by developing high SSA and refining the activation process of carbon. However, such attempts did not succeed. From a fundamental perspective, there is a clear lack of understanding of the double layer charging in the confined space of micropores, where there is no room for formation of Helmholtz layer and diffuse layer expected at a solid-electrolyte interface. EDL theory in such cases fails to describe the experimental observations. Therefore, and electric double-cylinder capacitor (EDCC) model is used for describing mesoporous carbon electrodes (Figure 7).

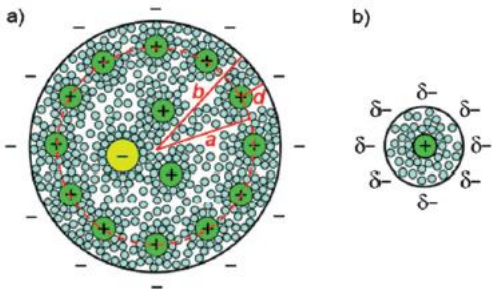

Figure 7: (a) A negatively charged mesopore with solvated cations approaching the pore wall to form a double-layer capacitor. (b) a negatively charged micropore of radius *b* with cations lining up along pore axis [1].

Pseudo-capacitance Mechanism: In contrast to EDL, pseudo-capacitance arises from purely thermodynamic reasons and is due to charge acceptance and a change in potential. The derivative $C = d(\Delta q)/(d\Delta v)$ is referred to as pseudo-capacitance. The major difference from EDL is that the pseudo-capacitance is faradic in origin, involving fast and slow redox reactions.

2.3.3 Performance criteria

The performance of supercapacitors is mainly evaluated on the basis of the following criteria: (a) a power density substantially greater than batteries with acceptably high energy densities; (b) an excellent cyclability; (c) fast charge/discharge process within seconds; (d) low self-discharging; (e) safe operation; and (f) low cost.

2.4 Lithium-ion batteries: Definition and working principles

A lithium-ion battery is a device comprising a graphite negative electrode (anode), a non-aqueous liquid electrolyte, and a positive electrode (cathode) formed from layered LiCoO2 (Figure 8). On charging, lithium ions are de-intercalated from the layered LiCoO2, pass across the electrolyte, and are in intercalated between the graphite layers in the anode. Discharge reverses this process. The electrons pass around the external circuit.

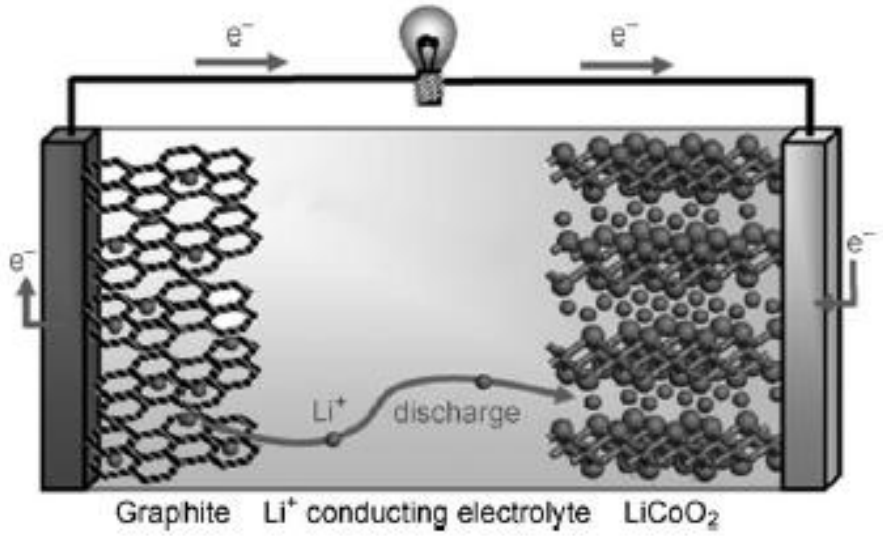

Figure 8: Schematic representation of a lithium-ion battery [5].

2.5 Solar/Photovoltaic cells and solar energy conversion

In order to meet the increasing energy demand, we will be forced to seek environmentally clean energy resources. Three major options that are at our disposal include carbon neutral energy, nuclear power, and renewable energy. Among these, solar energy stands out as the most viable choice to meet our energy expenditure. Although this option is ideal, it requires new initiatives to harvest incident photons with greater efficiency. The first generation photovoltaic devices suffer from high manufacturing cost and installation. The second generation polycrystalline semiconductor devices can bring down the cost, but their efficiency needs improvement. The field is now poised for third generation devices because of our ability to design nanostructures semiconductors, organic-inorganic hybrid materials, and molecular assemblies. The principles for some selected solar cells are discussed below briefly.

Photochemical Solar Cells: Various strategies have been developed in recent years to construct photochemical solar cells using organized assemblies of nanostructure architectures. Four promising strategies in this area are: (a) donor-acceptor based molecular clusters; (b) dye-sensitization of semiconductor nanostructures; (c) quantum dot solar cells; and (d) carbon nanostructure based solar cells. These systems are illustrated in Figure 9.

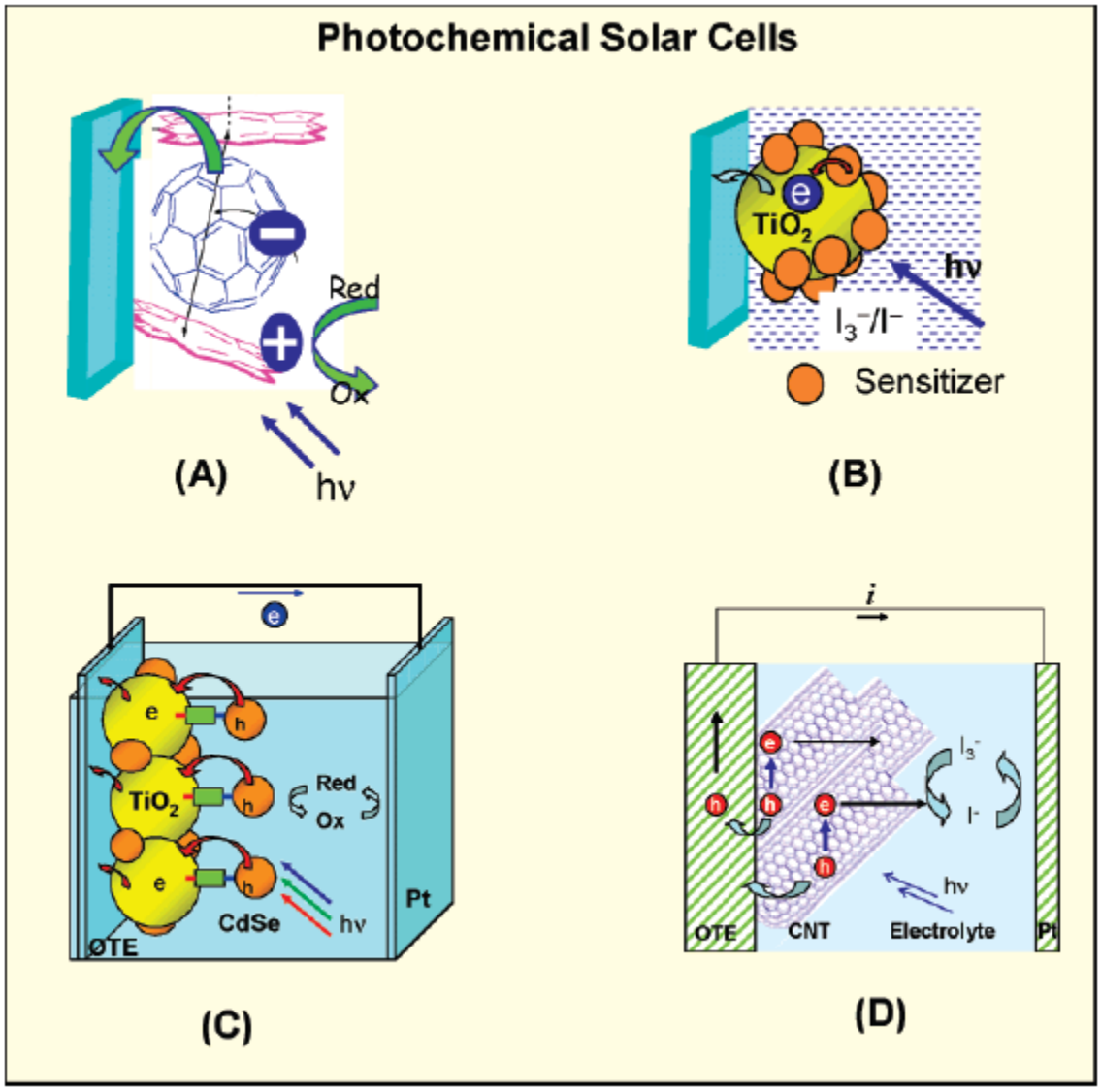

Figure 9: (a) Photo-induced electron transfer in donor-acceptor assemblies. (b) Charge injection from excited dye into semiconductor nanoparticles. (c) Photo-induced electron-hole separation. (d) Carbon nanotube architectures on electrode surfaces [8].

Principles of Dye-Sensitized Solar Cells: The process of utilizing sub-bandgap excitations with dyes is referred as photosensitization and is conveniently employed in photography and science imaging applications. The dye modified semiconductor provides an efficient method to mimic the photosynthetic process. The charge separation is facilitated by a semiconductor particle. The principle of working of a dye sensitized solar cell is shown in Figure 10.

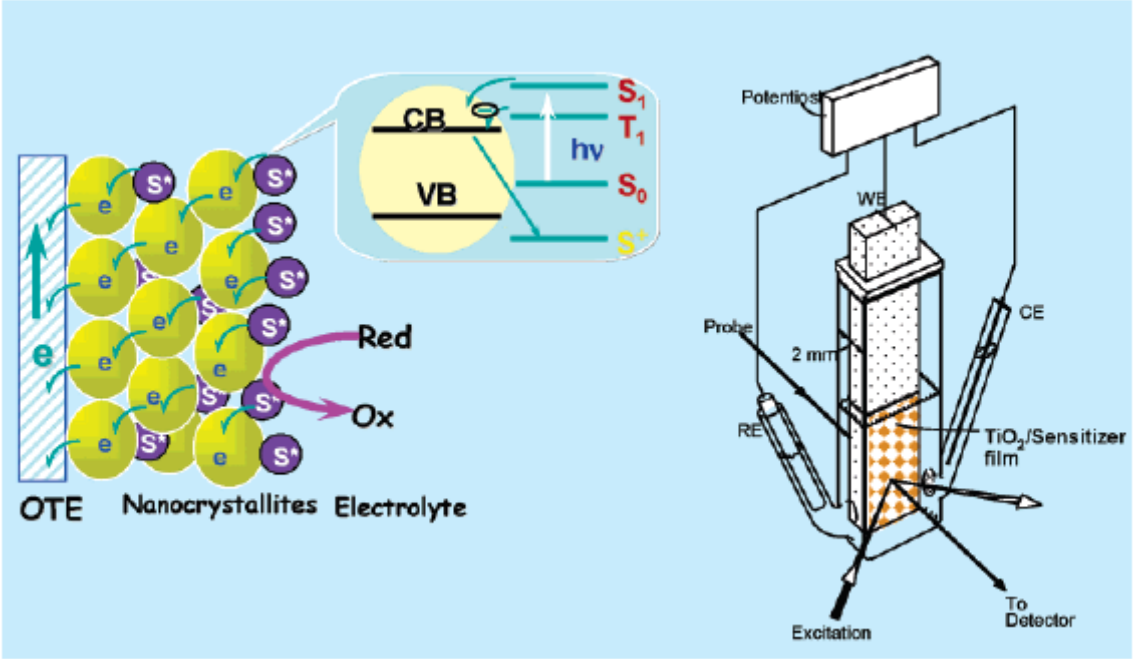

Figure 10: The scheme shows charge injection from excited sensitizer (S*) into semiconductor electrolytes. The design on the right shows a versatile cell assembly that is useful for electrochemical, spectroscopic, and spectroelectrochemical measurements [8].

Chapter 3: Nanomaterials for energy conversion and storage devices

3.1 Introduction

Significant progress is being made in the development of renewable energy technologies such as fuel cells, solar cells, and biofuels. Although a variety of renewable energy technologies have been developed and implemented, their wide-spread use is still highly limited. In order to achieve high performance in such technologies, it is essential to design sophisticated molecular level structures with different materials that offer enhanced properties for more efficient energy conversion and storage. New classes of materials composed of particles of nanometer dimensions, known as nanomaterials, have attracted great interest in recent years because of their unusual and unique electrical, mechanical, and optical properties. Nanostructured materials are becoming highly useful for electrochemical energy conversion and storage. The emergence of nanomaterials as the building blocks for energy harvesting assemblies has opened new ways for environmentally friendly and renewable energy sources. This chapter provides an overview of the state-of-the-art nanomaterials used in different energy conversion devices such as electrochemical capacitors, lithium batteries, and fuel cells, etc. The advantages and disadvantages of different nanomaterials used in energy conversion and storage devices will also be outlined.

3.2 Materials

In the following, materials for different energy conversion and storage devices are outlined briefly.

3.2.1 Materials for electrochemical supercapacitors

Carbon-based materials ranging from activated carbons, carbon aerogels, to carbon nanotubes (CNTs) are the most widely used electrodes in supercapacitors because of the often-cited desirable physical and chemical properties. Typical properties include low cost, variety of form (composites, sheets, and tubes), easy processability, inert electrochemistry, controllable porosity, etc. Templated porous carbons of microporous, mesoporous, and macroporous sizes with a tailorable structure are highly promising as supercapacitor electrode materials. Typically, higher power densities correlate with larger pore sizes, and higher energy densities with smaller pore sizes. EDLCs use carbon-based active materials with high surface area, while transition metal oxides as well as electrically conducting polymers are examples of pseudo-capacitive active materials. Carbon aerogels are continuous networks of conductive nanoparticles with interspersed mesopores. Carbon aerogels do not require the application of an adhesive binding agent because of their ability to bond chemically to the current collector. Carbon nanotubes based electrodes are grown as an entangled mat of carbon nanotubes with an open and accessible mesoporous network, which facilitates easier diffusion of ions. Hybrid capacitors, combining capacitive or pseudo-capacitive electrode with a battery electrode, are the latest types of EC, which benefit from both the battery and capacitor properties. More recently, graphene, a new class of two-dimensional carbon nanostructure, having large specific surface area and unusually high electronic qualities, is forecasted to have great potential in supercapacitor applications given that large-scale production of graphene sheets is possible. The most commonly studied materials include oxygen and nitrogen containing surface functional groups. The performance and physical properties

of some novel materials used as in various supercapacitor electrodes are summarized in Table 1.

Table 1 Properties and characteristics of various carbon and carbon-based materials as supercapacitors electrode materials

Materials	Specific surface area/$m^2\ g^{-1}$	Density/g cm^{-3}	Aqueous electrolyte		Organic electrolyte	
			/F g^{-1}	/F cm^{-3}	/F g^{-1}	/F cm^{-3}
Carbon materials						
Commercial activated carbons (ACs)	1000–3500	0.4–0.7	< 200	< 80	< 100	< 50
Particulate carbon from SiC/TiC	1000–2000	0.5–0.7	170–220	< 120	100–120	< 70
Functionalized porous carbons	300–2200	0.5–0.9	150–300	< 180	100–150	< 90
Carbon nanotube (CNT)	120–500	0.6	50–100	< 60	< 60	< 30
Templated porous carbons (TC)	500–3000	0.5–1	120–350	< 200	60–140	< 100
Activated carbon fibers (ACF)	1000–3000	0.3–0.8	120–370	< 150	80–200	< 120
Carbon cloth	2500	0.4	100–200	40–80	60–100	24–40
Carbon aerogels	400–1000	0.5–0.7	100–125	< 80	< 80	< 40
Carbon-based composite materials						
TC–RuO_2 composite	600	1	630	630	—	—
CNT–MnO_2 composite	234	1.5	199	300	—	—
AC–polyaniline composite	1000	—	300	—	—	—

3.2.2 Role of electrolyte

The performance of a supercapacitor is not only dependent on the electrode materials, but also on the electrolytes used. A high cell operating voltage provides both high energy density and power density, but is limited by the stability of the electrolyte in the applied potential. The most recent supercapacitors use electrolytes based upon aprotic solvents and typical carbonate-based solvents. Figure 11 shows the advantages of a higher energy density when using aprotic vs aqueous electrolyte. However, there are other considerations on the use of non-aqueous solvents such as high cost, low conductivity, low dielectric constant, as well as safety. It is worth noting that there are two main factors involved in the conductivity of the electrolyte system: (a) the ability of the salt dissociation; and (b) the mobility of the dissociated ions in the electrolyte system.

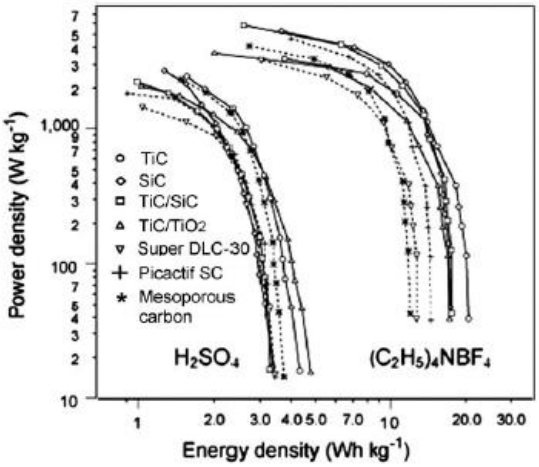

Figure 11: Ragone plots for comparison for the performance of various types of carbon electrodes in aqueous and aprotic electrolytes.

3.2.2 Materials for pseudocapacitors

As described in Chapter 2, pseudocapacitors store charge Faradaically through the transfer of charge between the electrode and electrolyte. This is typically accomplished through electrosorption, and reduction-oxidation reactions. The most commonly known active species used as electrode materials are conducting polymers, ruthenium oxide, manganese oxide, and vanadium nitride. It is known that ruthenium oxide pseudocapacitors are likely to achieve higher energy and power densities than conducting polymer based pseudocapacitors. However, the costs associated with such materials are relatively high.

3.3 Materials for Lithium-ion batteries

Although Lithium-ion batteries are commercially successful, we are reaching the limits in performance using the current electrode and electrolyte materials. For new generation of

batteries, significant breakthroughs in materials chemistry are essential. Particularly, an increase in the charge/discharge rate of lithium-ion batteries of more than an order of magnitude is required for future applications in hybrid electric vehicles, and clean energy storage. Nanomaterials have the genuine potential to make a significant impact on the performance of such batteries because their reduced dimensions allow high rates and high power. However, there are many advantages and disadvantages of nanomaterials in battery applications.

Advantages

1. They enable electrode reactions to occur that cannot take place for materials composed of micrometer-sized particles.
2. The reduced dimensions increase significantly the rate of lithium insertion/removal, because of the short distances for lithium-ion transport within the particles.
3. Electron transport within the particles is also enhanced by nanometer-sized particles.
4. A high surface area permits a high contact area with the electrolyte and hence a high lithium-ion flux across the interface.
5. For very small particles, the chemical potentials for lithium ions and electrons may be modified, resulting in a change of electrode potential.
6. The range of composition over which solid solutions exist is often more extensive for nanoparticles.

Disadvantages

1. Nanoparticles may be more difficult to synthesize and their dimensions may be difficult to control.
2. High electrolyte/electrode surface area may lead to more significant side reactions.

3. The density of a nanopowder is generally less than the same material formed from micrometer-sized particles. The volume of the electrode increases for the same mass of material thus reducing the volumetric energy density.

3.4 Strategies for novel battery materials

Although nanomaterials are favorable in terms of kinetics and capacity, their practical applications suffer from low thermodynamic stability and high activity towards surface reactions besides handling problems, all of which are due to their small sizes. Described below are different types of novel materials.

Self-assembled nano/micro materials: Self-assembled nanostructure, i.e., a higher-level structure assembled from nanometer-sized building blocks including nanoparticles, nanorods, and nanofilms, is one of the hierarchical structure with great interest in the field of lithium-ion batteries promoted by the rapid advancement in synthetic strategies. Many facile solution based methods exist in the literature. For example, a polyol-process to synthesize V_2O_5 with highly ordered superstructures, in which nanoparticles interconnect to form nanorods, and these rods circle around to form hollow microspheres.

Nanostructured composites: Lithium alloys are promising anode materials due to their higher Li storage capacity, which provides higher energy density than commercial Li-intercalated carbons. The biggest challenge for alloy systems is that they are suffering from huge volume variation, which leads to rapid capacity decay. One solution to solve the problem is the active-inactive nanocomposite strategy, which consists of active nanoparticles that can alloy with Li and inactive matrix that not only acts as a buffer but also prevents aggregation of the nanoparticles upon cycling. Sn-C composites can

effectively alleviate the electrode pulverization problem. Another solution is to put nanometer- sized active particles into a hollow inactive container.

Mesoporous materials: There has always been a need for developing highly porous electrode materials with large surface areas. In this context, more emphasis should be on synthesis of optimized pore sizes and connectivity rather than striving for micro-pores ordered arrangements.

In addition to these materials, an optimized nanostructure design of electrode materials for high energy and high power batteries is the introduction of 3D mixed conducting networks on both nanoscale and microscale levels. Some of these strategies are summarized in Figure 12.

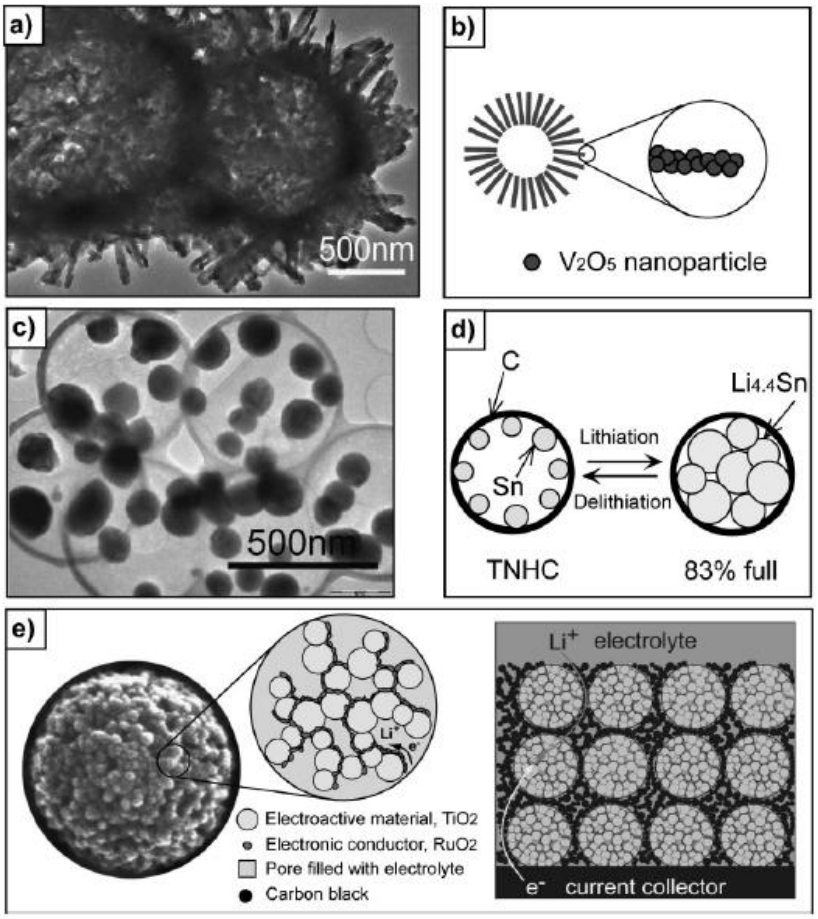

Figure 12: (a) TEM image and (b) schematic illustration of V2O5 hollow microspheres. (c and d) TEM image and illustration for tin nanoparticles encapsulated with elastic hollow carbon spheres. (e) Schematic illustration of 3D mixed conducting networks [7].

3.4 Materials for Solar/Photovoltaic devices

There are three ways in which one can utilize nanostructures for the design of solar energy conversion devices (Figure 13). The first one is to mimic photosynthesis with donor-acceptor molecular assemblies and clusters. The second one is the photo-catalysis assisted by semiconductors to produce fuels such as hydrogen. The third and most promising is the nanostructure semiconductor based solar cells.

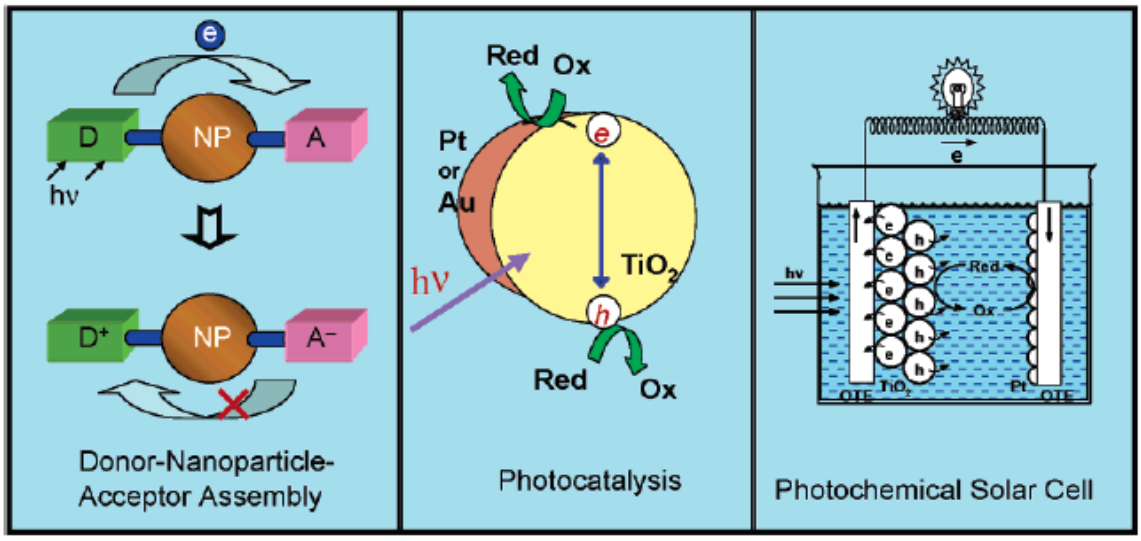

Figure 13: Strategies to employ nanostructured assemblies for light energy conversion for photovoltaic applications [8].

Donor-acceptor hybrid assemblies: In photosynthesis, light energy is converted into chemical energy by green plants. Based upon this principle, a variety of donor-acceptor dyads and triads have been synthesized as light harvesting assemblies. Of particular

interest are Chlorophyll and porphyrins that mimic the photoinduced electron-transfer process of natural photosynthesis. For example, porphyrin-alkanethiolate monolayer protected gold-nanoparticles (Figure 14) form spherical shape clusters that can be employed as light harvesting antenna. They exhibit efficient light-harvesting capability and suppress undesirable energy transfer quenching of the porphyrin.

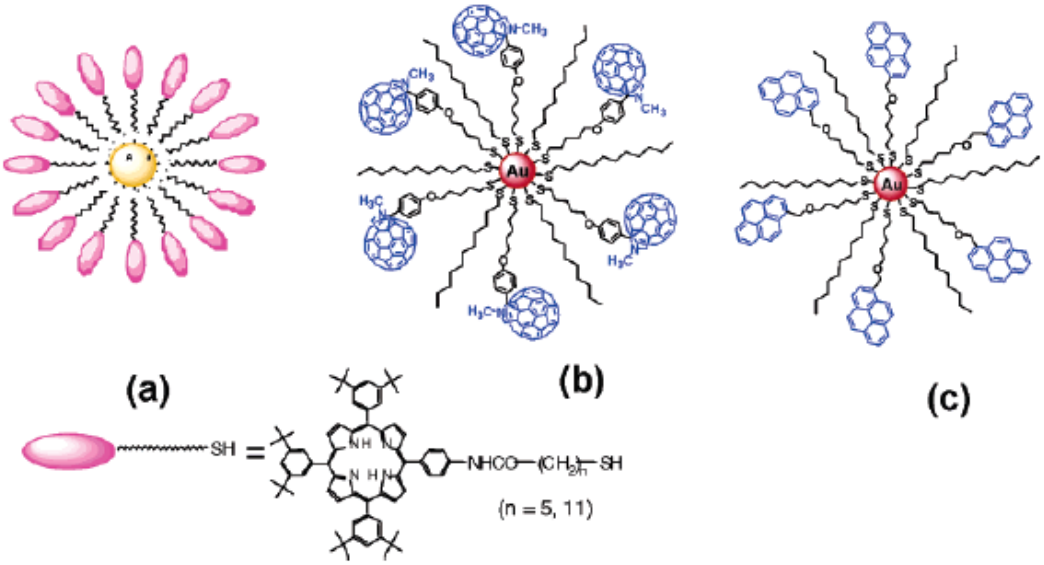

Figure 14: Examples of gold-nanoparticles functionalized with (a) porphyrin, (b) C60, and (c) pyrene [8].

Catalysis with Semiconductor Nanocomposites: Small size semiconductor particles can be utilized to induce redox processes at the interface. The photocatalytic processes using TiO2 and other semiconductors have demonstrated the need to overcome the limitations in achieving higher conversion efficiencies. Of specific interest in this context is the use of nanostructures for solar hydrogen production by photocatalytic splitting of

water. The principle of photocatalysis for producing solar hydrogen is presented in Figure 15.

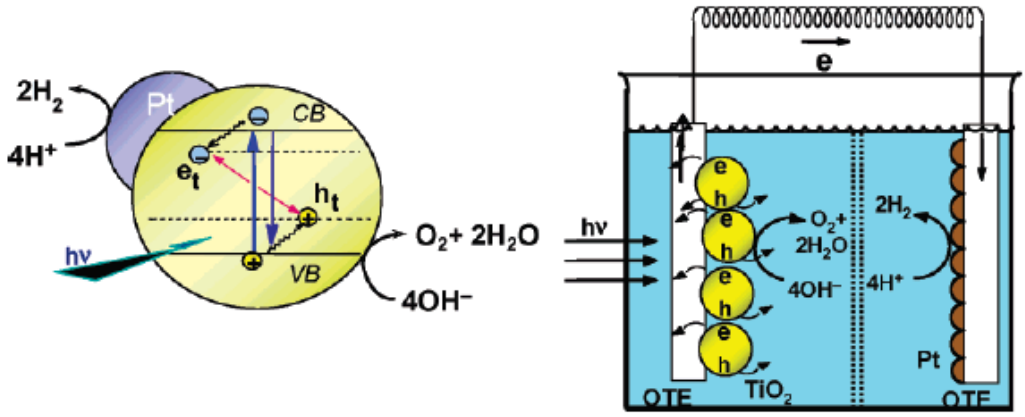

Figure 15: Photocatalytic splitting of water following the band gap excitation of the semiconductor nanoparticles (left) and a photo-electrolysis cell (right) [8].

Chapter 4: Modeling techniques for supercapacitors

4.1 Introduction

Several unique features of supercapacitors such as high power, high energy density, and reliability allow the use of these storage devices in a variety of applications [11]. To assist in reducing the cost and time required for fabrication and physical experimentation, it is often required to conduct quantitative modeling to predict performance characteristics of supercapacitors [12]. Such modeling is significantly helpful in developing supercapacitor systems that perform closer to theoretical limits. Several different types of models have been developed for supercapacitors that are sufficiently accurate, but they are often difficult to adapt for varied applications [11]. There are very few models that account for temperature dependence and aging effects. Designing a specific application requires implementation of key elements in the most appropriate mathematical form. Some of these models are discussed in the following.

4.2 Type of models

In broader terms, there are two different types of models that are developed for supercapacitors. The first type of model is known as equivalent circuit or RC circuit model, that employs mathematical or computer models of fundamental electric circuit components, such as capacitors and resistors, for modeling of electrochemical processes. These models have been traditionally used to predict performance characteristics of porous electrodes, and also have been applied to capture the interfacial behavior between the pores of electrodes and electrolyte solution. Similar models have also provided information on Faradaic effects observed in pseudo-supercapacitors. Figure 16 shows the

hierarchy of equivalent circuits used to model porous electrodes [12]. This begins with a simple capacitor and other components are added to reach a complete RC circuit model. In the final model, the distributed resistances represent the equivalent series resistance, and distributed capacitances are non-Faradaic double-layer capacitance of each pore. It is also possible to modify this equivalent circuit to models a porous pseudocapacitor electrode by incorporating the Faradaic pore equivalent circuit.

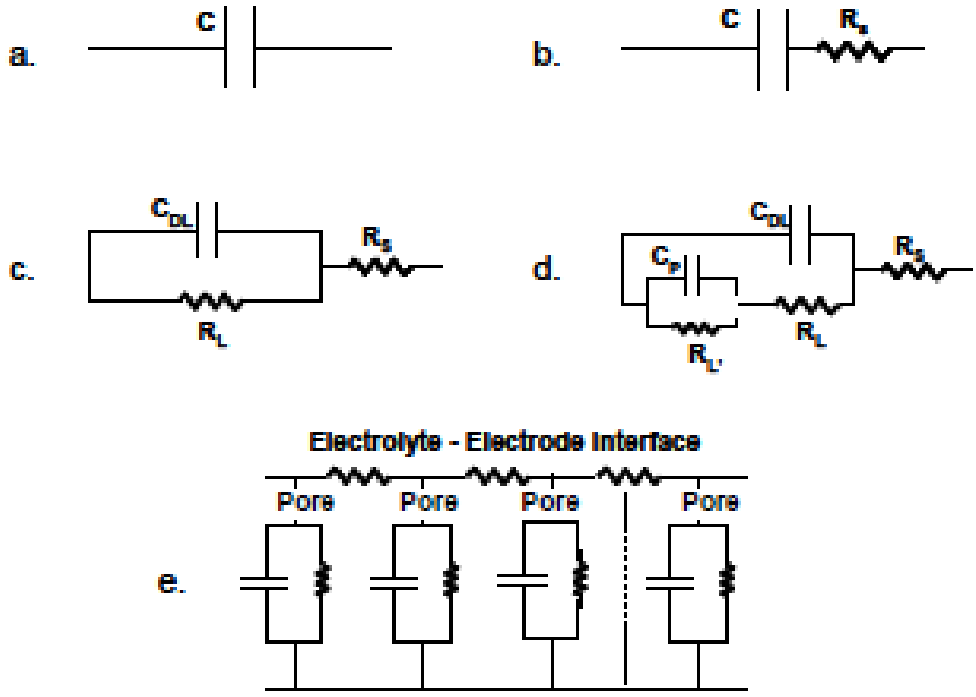

Figure 16: Equivalent circuit model hierarchy. (a) Simple capacitor; (b) capacitor with a series resistance; (c) capacitor and leakage resistance in parallel with a series resistance; (d) pseudocapacitor circuit that adapts (c) by adding a parallel circuit consisting of a

capacitor in parallel with leakage resistor; (e) transmission line model with has circuits of type (c) in parallel [12].

However, the equivalent circuit models do not easily relate to many physical processes such as ion transport in voids in response to applied electric field and charge buildup in the double layer [13]. In order to better understand such processes, we need to develop different types of models such as fundamental transport models that explicitly account for such diffusion effects. These transport models can be 1dimensional and 2 dimensional. Shown below in Figure 17 is a schematic of a supercapacitor cell for a transport model [14].

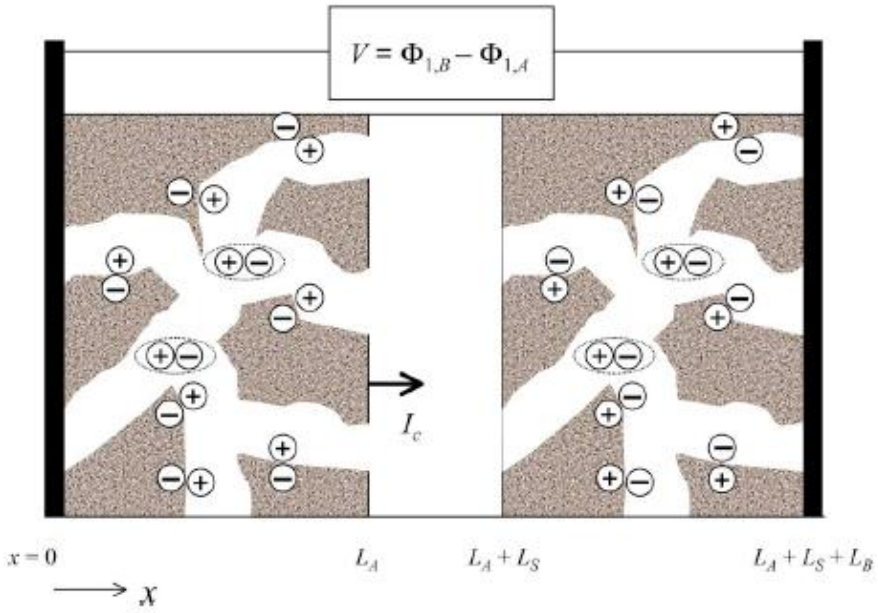

Figure 17: Schematic of a cross section of a supercapacitor cell. The dark regions are activated carbon while the white region is free electrolyte. Ions adsorbed on the electrode surface are balanced by the surface charge on the carbon electrode.

The model equations governing this type of supercapacitor model are presented in Figure 18.

Boundary conditions

Current collector $x = 0$	Electrode - separator boundary $x = L_A$	Electrode - separator boundary $x = L_A + L_S$	Current collector $x = L_A + L_S + L_B$
$\Phi_1 = 0$	$\left.\frac{\partial \Phi_1}{\partial x}\right\|_L = -\frac{i - i_2}{\sigma}$	$\left.\frac{\partial \Phi_1}{\partial x}\right\|_R = -\frac{i - i_2}{\sigma}$	$\frac{\partial \Phi_1}{\partial x} = -\frac{i - i_2}{\sigma}$
$\frac{\partial \Phi_2}{\partial x} = -\frac{i_2}{\kappa}$	$\left[\kappa \frac{\partial \Phi_2}{\partial x} + \kappa\left(\frac{t_+ - t_-}{f}\right)\frac{\partial \ln c}{\partial x}\right]_L = \left[\kappa \frac{\partial \Phi_2}{\partial x} + \kappa\left(\frac{t_+ - t_-}{f}\right)\frac{\partial \ln c}{\partial x}\right]_R$	$\left[\kappa \frac{\partial \Phi_2}{\partial x} + \kappa\left(\frac{t_+ - t_-}{f}\right)\frac{\partial \ln c}{\partial x}\right]_L = \left[\kappa \frac{\partial \Phi_2}{\partial x} + \kappa\left(\frac{t_+ - t_-}{f}\right)\frac{\partial \ln c}{\partial x}\right]_R$	$\frac{\partial \Phi_2}{\partial x} = -\frac{i_2}{\kappa}$
$i_2 = 0$	$i_2 = i$	$i_2 = i$	$i_2 = 0$
$\frac{\partial c}{\partial x} = 0$	$D\left.\frac{\partial c}{\partial x}\right\|_L = D\left.\frac{\partial c}{\partial x}\right\|_R$	$D\left.\frac{\partial c}{\partial x}\right\|_L = D\left.\frac{\partial c}{\partial x}\right\|_R$	$\frac{\partial c}{\partial x} = 0$

Field equations

Electrode, $0 \le x \le L_A$	Separator, $L_A \le x \le L_A + L_S$	Electrode, $L_A + L_S \le x \le L_A + L_S + L_B$
$\frac{\partial \Phi_1}{\partial x} = -\frac{i - i_2}{\sigma}$	…	$\frac{\partial \Phi_1}{\partial x} = -\frac{i - i_2}{\sigma}$
$\frac{\partial \Phi_2}{\partial x} + \left(\frac{t_+ - t_-}{f}\right)\frac{\partial \ln c}{\partial x} = -\frac{i_2}{\kappa}$	$\frac{\partial \Phi_2}{\partial x} + \left(\frac{t_+ - t_-}{f}\right)\frac{\partial \ln c}{\partial x} = -\frac{i_2}{\kappa}$	$\frac{\partial \Phi_2}{\partial x} + \left(\frac{t_+ - t_-}{f}\right)\frac{\partial \ln c}{\partial x} = -\frac{i_2}{\kappa}$
$\frac{\partial i_2}{\partial x} = aC\frac{\partial (\Phi_1 - \Phi_2)}{\partial t}$	$i_2 = i$	$\frac{\partial i_2}{\partial x} = aC\frac{\partial (\Phi_1 - \Phi_2)}{\partial t}$
$\varepsilon_2 \frac{\partial c}{\partial t} = D\frac{\partial^2 c}{\partial x^2} - \frac{aC}{F}\left(t_- \frac{dq_+}{dq} + t_+ \frac{dq_-}{dq}\right)\frac{\partial (\Phi_1 - \Phi_2)}{\partial t}$	$\varepsilon_2 \frac{\partial c}{\partial t} = D\frac{\partial^2 c}{\partial x^2}$	$\varepsilon_2 \frac{\partial c}{\partial t} = D\frac{\partial^2 c}{\partial x^2} - \frac{aC}{F}\left(t_- \frac{dq_+}{dq} + t_+ \frac{dq_-}{dq}\right)\frac{\partial (\Phi_1 - \Phi_2)}{\partial t}$

Figure 18: Governing equations with boundary conditions. The boundary conditions on the current collectors imply that all current resides in the solid phase at the current

collectors and no ions enter the current collectors. The potential at left current collector is set to zero. The cell potential is given by Φ_1 at the right current collector, and Φ_2 represents a solution-phase potential. There is no solid phase in the separator region, and at the electrode-separator boundary, all current is transferred to solution phase. The cell current, power, and the potential are the parameters that are controlled. Subscripts L and R refer to left and right, respectively, for the gradient terms, *c* is the concentration, and *D* the diffusion coefficient. The currents are represented by *i*, and i_1 and i_2, respectively, are currents in the solid and solution phase.

The equivalent circuit models can be solved by a variety of software such as Simulink, while the transport model equations above can be solved using software such as COMSOL. A brief description of such software is presented in the following section.

4.3 Software for modeling supercapacitors

There are a variety of software programs that are commercially available to carry out quantitative modeling of supercapacitors, and these programs have been analyzed and compared previously [15]. These programs have a typical graphical user interface to start building models, where the user can add/delete different components, and the details on program functionalities can be located in the Help functions of software. In the following, these programs and their features are briefly highlighted.

4.3.1 Simulink

Simulink is a software package that is a part of program MATLAB, and it can simplify modeling and simulation analysis in comparison to direct code-based modeling in MATLAB. There are various mathematical blocks and signal handling blocks that are

available in Simulink, which can be used to model more specific complex models. One disadvantage of these blocks is that the user needs to predetermine the type of input such as current or voltage, because it is not possible to use the same circuit model for both types of input parameters. The MathWorks also provides different types of toolboxes and application to further increase functionalities of Simulink and MATLAB. Some of the examples are Statistics toolbox, Math toolbox, control system toolbox, etc. Some other toolboxes that can be combined with Simulink are SimPowerSystems, SimDriveline, and SimHydraulics. Some of these toolboxes are dependent on a third toolbox named Simscape. Simulink also allows addition of a key component known as the Parameter Estimation Tool, which helps in finding values of specific model parameters that are consistent with measured results.

User interface for Simulink: The components in Simulink are combined in a large library which is arranged in sub-groups. Some of these groups can be input, output, and logic, etc. One can use any of the available signals as input, and manipulate these using different blocks. It is also possible to combine several signals into one signal line, which both saves space as well as improves the model overview. If one can develop small sub-models in Simulink, they can used again to make different complex models.

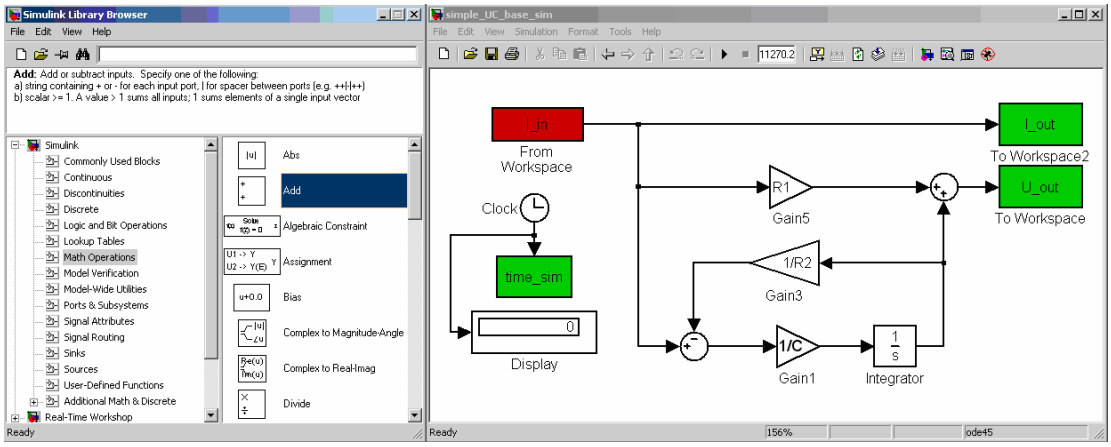

Figure 19: User interface for Simulink [15].

4.3.2 SimPowerSystems

SimPowerSystems is an additional toolbox that can be added to Simulink component library for modeling of electrical circuits using standard symbols. The available circuit components can be capacitors, resistors, transformers, and other power electronics components such as AC/DC electric drives. Component support to model different battery types of batteries is also present in some versions of this program. Unlike Simulink, it is possible to switch model input from voltage to current without altering the modeled circuit, which is a big advantage. The program also has a specific graphical user interface for analysis of circuits and systems which is known as *powergui*. The help functions are detailed and provide information on how various aspects are modeled, and how modeling is to be carried out.

User interface for SimPowerSystems: As pointed out above, SimPowerSystems is toolbox that works with Simulink. Therefore, same workspace as in Simulink can be used for modeling. The only difference is addition of additional components in the existing library. It is powerful because mathematical components in Simulink now can be combined with electrical components for direct circuit design. The model design starts by linking together Simulink components with electrical components, and getting a mathematical description of the modeled system. These mathematical equations are then solved by ordinary differential equation (ODE) solver in MATLAB. It is possible to carry out not only continuous simulation but also discrete simulation with small time-step integration. It is particularly useful for very large systems where continuous simulation

can result in too long simulation, and discretization is often required. The user interface for this program is shown in Figure 20.

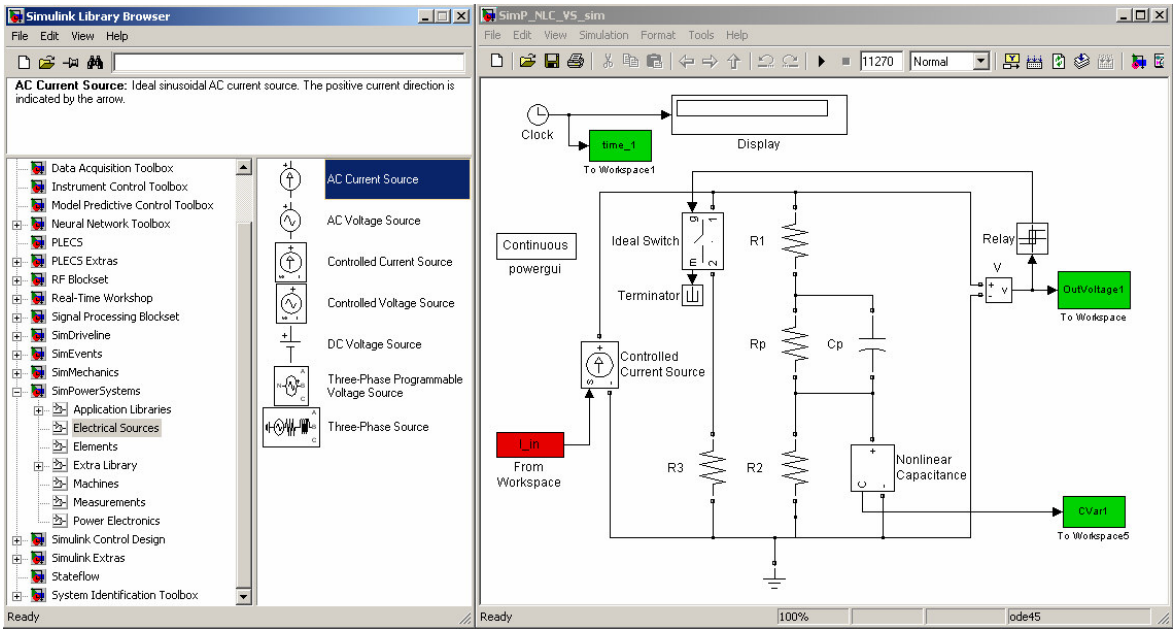

Figure 20: User interface for SymPowerSystems.

4.3.3 OrCAD Capture

This program is primarily meant for electrical circuit design and simulation. One cannot create models for other domains due to this reason. One can combine this program with Simulink using a third helper program called SLPS, which enables usage of models created using OrCAD Capture with model systems in Simulink. Like other programs, libraries are available for creating circuits with different components. Simulation calculation and result plotting is done using program PSpice.

User interface for OrCAD Capture: Components in the user interface of this program are found grouped in libraries, where one library has similar types of functions and applications. The left part of interface has an overview of the project, while the right part has detailed schemes (Figure 21).

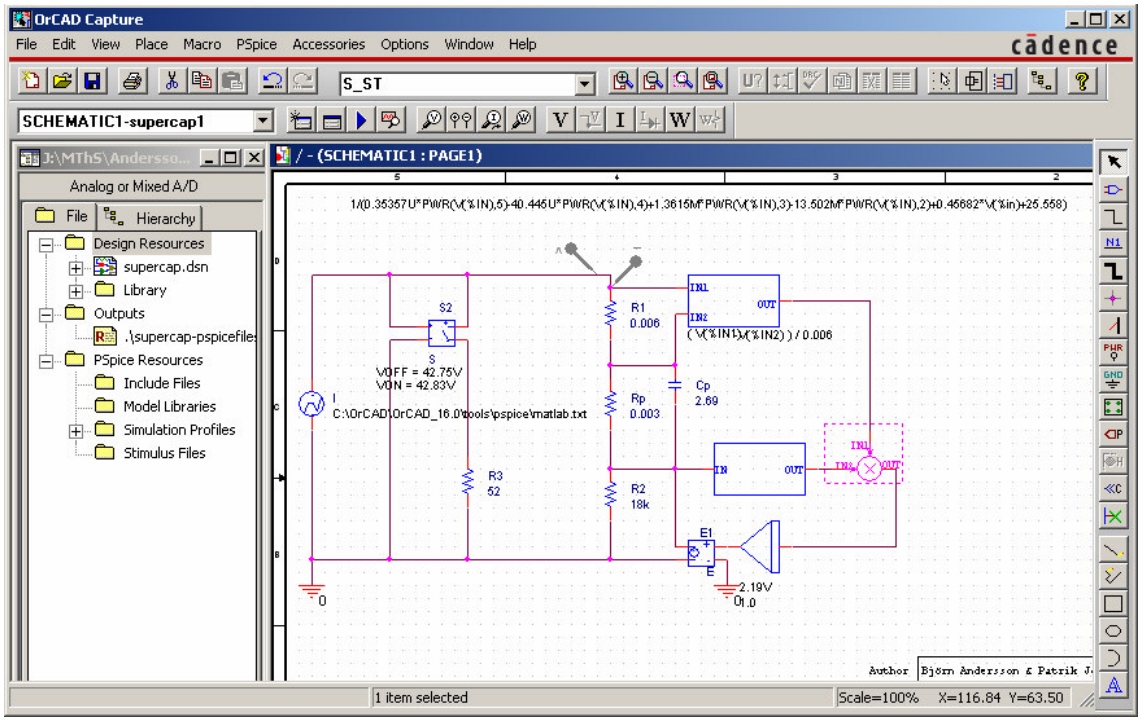

Figure 21: User interface for OrCAD Capture.

4.3.4 PSCAD

This program is used for AC/DC power simulations. The main purpose of this program is to create electrical circuits and analyze electromagnetic transients using simulations. This program can also be combined with MATLAB/Simulink environment using specific FORTRAN based code [15].

User interface for PSCAD: Similar to some other programs, it is possible to create electrical circuits by choosing various components. Once the circuit is constructed, it can be simulated and results can be analyzed in the workspace area via graphs. The user has the flexibility of altering the model during a simulation, and specific blocks in the component library are available to carry this out. There is also no restriction on whether components are connected in series or parallel. The user interface for this program is shown in Figure 22.

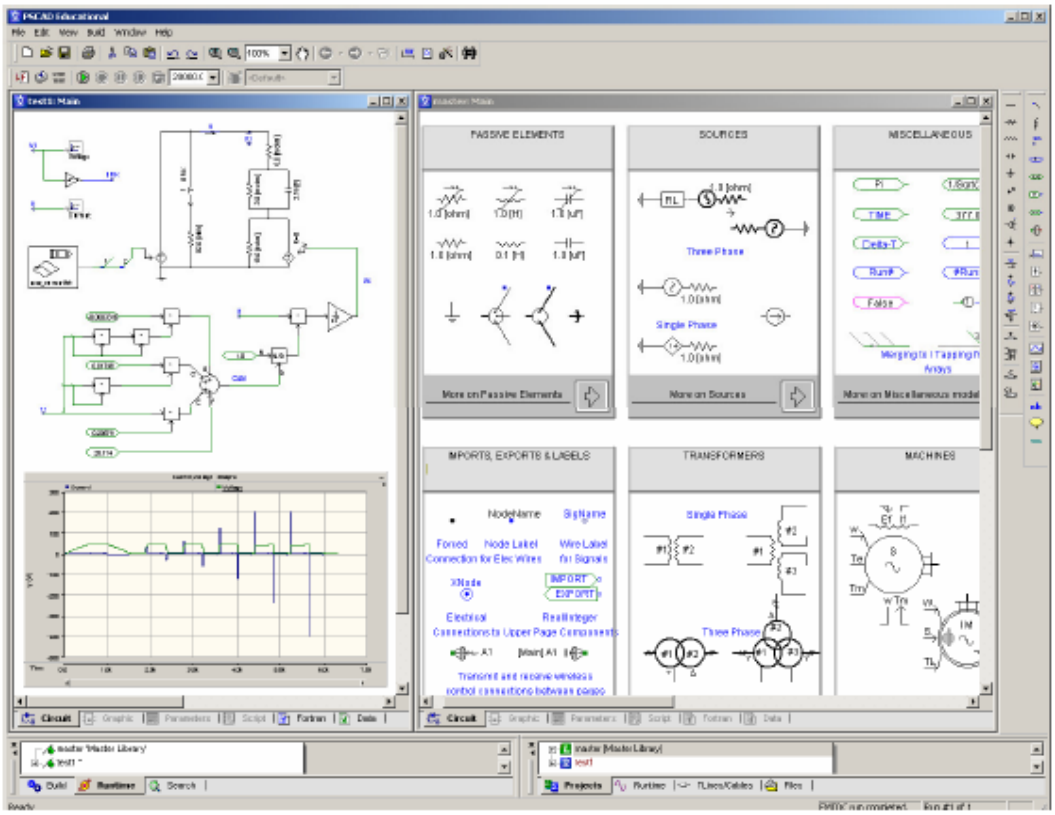

Figure 22: User interface for PSCAD.

4.3.5 Saber

Saber is a powerful program that allows simulations of physical effects in many engineering domains such as electrical, mechanical, thermal, and hydraulic. This program includes a large model library as well as tools for advanced analysis such as Monte Carlo and Sensitivity. Due to advanced tools, it is possible to model entire vehicles in Saber. Various analyses such as small-signal frequency analyses and time-domain transient analysis can be done. This program is popular in automotive, aerospace, and power industries. Various components that are present include electrical motors, batteries, sparkplugs, fuel cell stacks, hydraulic pumps, and valves. Saber also contains a model of supercapacitor in the Parts Gallery. This model also includes a series resistance that is temperature-dependent thereby allowing modeling of temperature as a parameter. A tool called SaberRT is available for real-time simulation of Saber designs. Special tools can be used as interface for programs such as Simulink, ModelSim, and Verilog.

User interface for Saber: The parts gallery is displayed on left the user interface of this program and is classified based upon application. Each library can contain thousands of parts that are easy to locate. These parts can be searched using search terms or browsing quickly through various categories. The alphabetical list of parts is also available. The user interface is somewhat old and is shown in Figure 23.

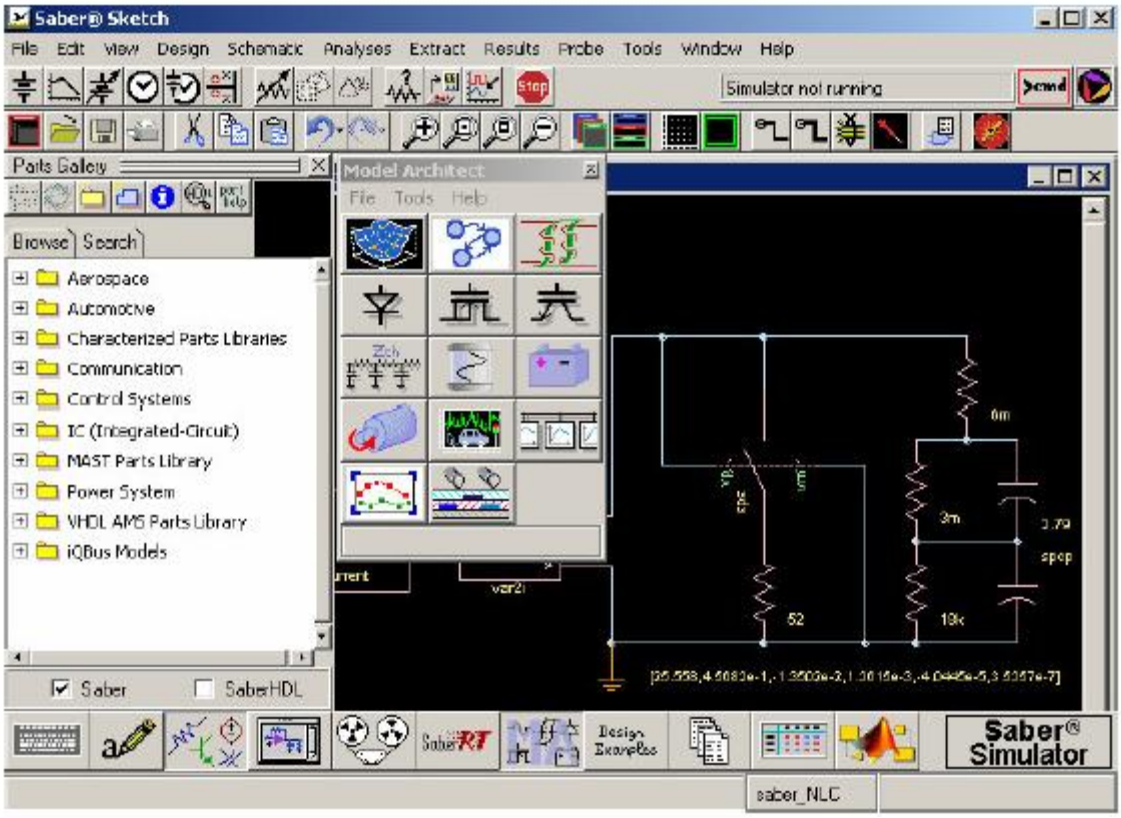

Figure 23: User interface for Saber.

4.3.6 PLECS

PLECS is a toolbox for electrical circuits in Simulink but is not a product of MathWorks. It makes use of calculation methods used in MATLAB for solving equations of electrical components, and models. This program is easy to integrate with Simulink, and significantly help in simplifying circuit design. A library of non-linear components is also available, and a library with thermal elements to model temperature-dependent phenomenon is present.

User interface for PLECS: This is very similar to SimPowerSystems. The workspace contains the electrical components that are connected by wires and can be used with

Simulink modeling. The components are arranged in various libraries classified based upon application areas. Libraries of both ordinary components such as resistors and advanced components such as drives are present. The user interface is shown in Figure 24.

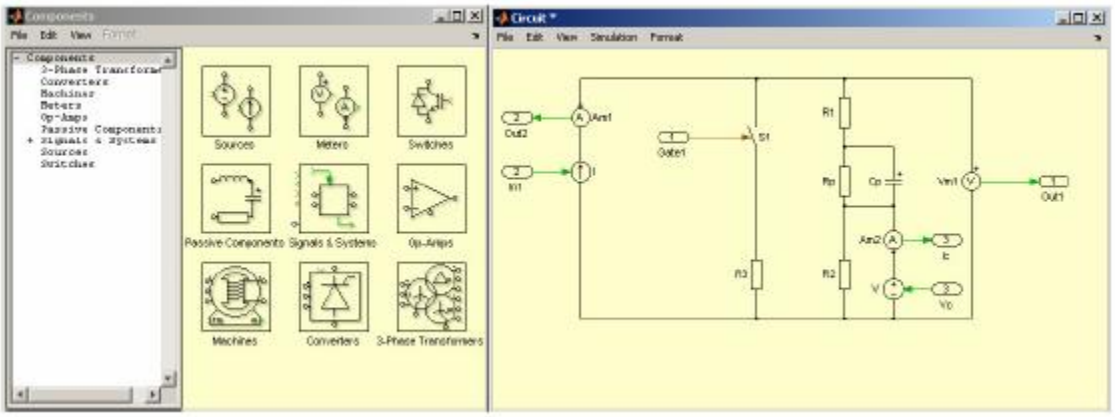

Figure 24: User interface for PLECS.

4.3.7 Dymola

Dymola is a graphical user interface for Modelica language, which can be used to model physical processes. In this program, mechanical, electrical, thermal, control, and hydraulic components can be combined together. The modeling can be done either using the user interface or by writing a code. Dymola blocks can also be used in the Simulink environment.

User interface for Dymola: The models like any other software are built using components that are picked from libraries. The component window is at the bottom left (Figure 25). It is possible to run simulation and export results in various image formats.

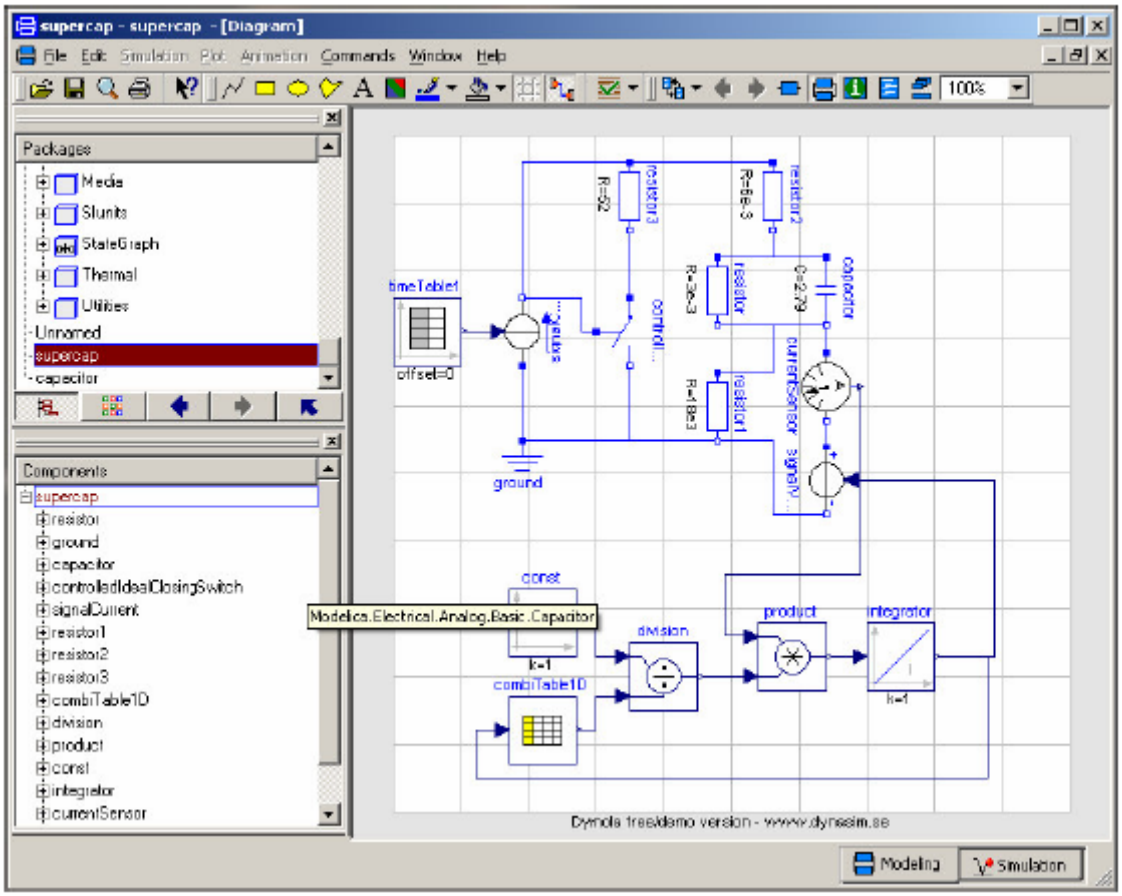

Figure 25: User interface for Dymola.

4.4 Advantages and disadvantages of various software programs

4.4.1 Simulink

Advantages: Simulink has a large user base due to MATLAB usage, and Help functions are well structured. Any control algorithm can be implemented using a variety of library routines, and parameter estimation is also available.

Disadvantages: A big disadvantage is reduced performance of simulation compared with modeling done using a direct code. Additionally, one can only carry out mathematical modeling, and electrical modeling like many other programs is not as sophisticated in terms of model overview.

4.4.2 SimPowerSystems

Advantages: It is possible to carry out electrical modeling, and comprehensive documentation is available on various components. Because it is a toolbox, one has a direct access to MATLAB and Simulink environments.

Disadvantages: Models at times only include partial behavior of actual components, and only electrical modeling is possible. There can also be issues with how capacitors are connected.

4.4.3 OrCAD Capture

Advantages: This program allows fast and intuitive editing, and also increase efficiency of editing by resuse of design. It also contains a large library of electrical components, and includes many electrical parts.

Disadvantages: The help function is not descriptive enough and contains only incomplete information on different parts. The program is only suitable for circuit design.

4.4.4 PSCAD

Advantages: The help function is detailed and provides relevant information. Many different electrical parts are available along with a large library of electrical components. Altering the model during simulation is possible and results can be plotted.

Disadvantages: A fixed step can only be used during simulation.

4.4.5 Saber

Advantages: The largest component library is available, and it is possible to do multi-domain simulations. The Help function is detailed, and co-simulation with Simulink are possible. It also includes and advanced supercapacitor component. Analyses tools are powerful

Disadvantages: The user interface is old.

4.4.6 PLECS

Advantages: Components are well organized and direct access to MATLAB and Simulink is available. Thermal modeling is also possible as well as non-linear components can be used.

Disadvantages: Analysis of results is not as good as SimPowerSystems. Only electrical domain simulation is possible.

4.4.7 Dymola

Advantages: Equation-based modeling can be carried out, and multi-domain simulation is also possible. Several additional libraries are also present.

Disadvantages: The program is limited in terms of export formats, and analysis of results.

4.5 Basic model of a supercapacitor

In the following, a basic model of supercapacitor is presented, and its Simulink version implementation is shown. A supercapacitor can be easily modeled using some simple circuit components such as a voltage source, capacitor, and a resistor. A conceptual circuit is shown in Figure 26.

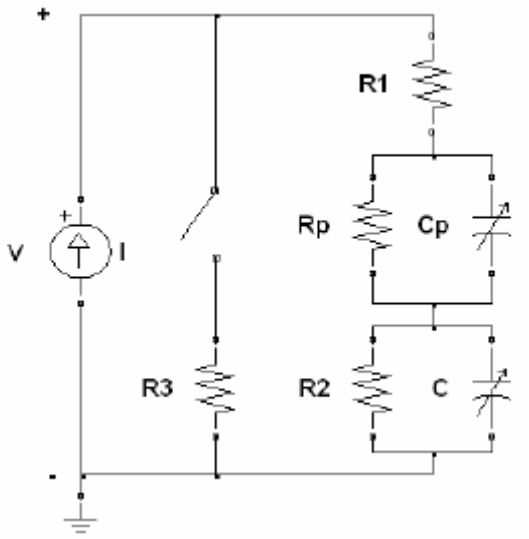

Figure 26: The basic circuit model of a supercapacitor [15].

In the above model, the two variable capacitances are nonlinearly varying with the voltage that is applied across the circuit. The capacitance *C* is the most important parameter in the model because it determines how the charge is handled, the amount of energy stored, and the rate of energy level variations. The resistance R2 is connected to

represent self-discharge, while R1 represents the losses during charge/discharge. The losses occur because conducting elements in the supercapacitor has a resistance. R3 provides the voltage protection and switch is necessary to prevent damage to the capacitor. The resistance Rp and capacitance Cp are present to model the fast dynamics in the behavior of the supercapacitor.

4.5.1 Simulink model

A Simulink based implementation of the model described above is shown in Figure 27.

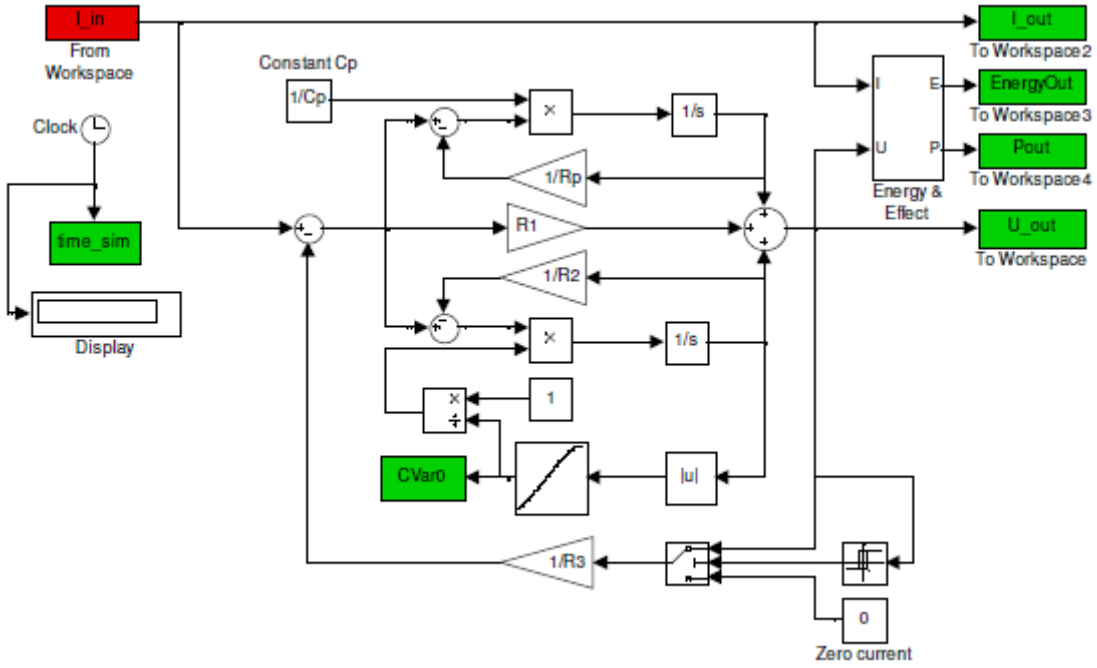

Figure 27: Simulink implementation of basic supercapacitor model with variable capacitance.

Initial model implementation is done with a simple circuit consisting of resistance in series with a capacitance and resistance in parallel. This basic implementation can show fundamental function of a supercapacitor. The relay block controls the switch that

connects the balancing resistance R3. The protection is provided by a voltage control because supercapacitors are sensitive to over-voltage. The initial values of capacitances and resistances are taken from measurements or data tables. Typical values are R1 = 6 mΩ; R2 = 18 kΩ; R3 = 52 mΩ; R_p = 3 mΩ; C = 35F; and C_p = C/13. An output voltage curve is shown in Figure 28.

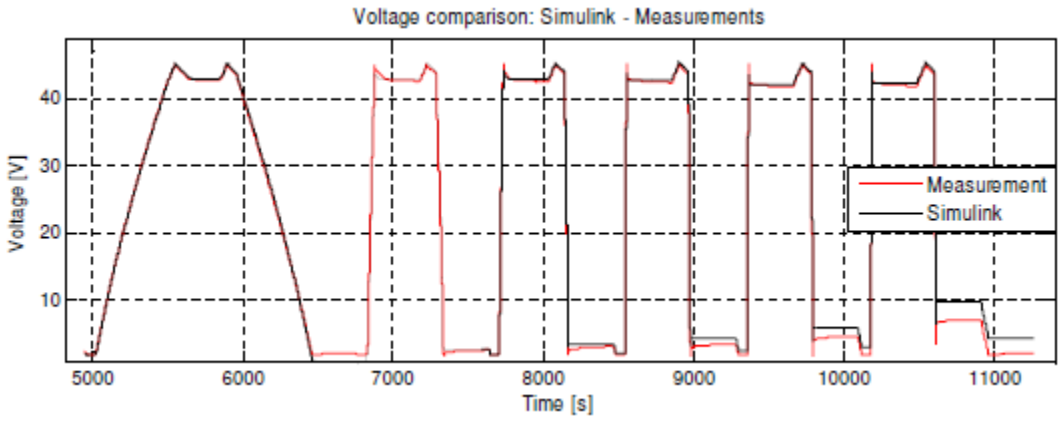

Figure 28: Voltage curve for basic model with nonlinear capacitance.

The effect of over-voltage balance is visible in the above plot. The resistance is connected when voltage value is ~42V, and due to which the model voltage does not overshoot.

4.6 Consideration in choosing the proper model

Before testing any simulation program, various considerations needs to be taken into account in choosing a proper model. Some of these considerations may include frequency and temperature dependence of capacitance and resistance. Typically, series resistance increases with decreasing temperature, and capacitance variation with voltage introduces a nonlinear component. At the same voltage, at different temperatures, the capacitance

varies more in the charging state. Therefore, care should be taken in using various models for quantitative understanding of supercapacitor behavior in various states.

Chapter 5: Modeling techniques for photovoltaic cells

5.1 Introduction

A photovoltaic (PV) cell converts the solar energy into electrical energy by photovoltaic effect. In other words, a PV cell is a semiconductor diode whose p-n junction is exposed to light. The PV cells are typically operated at their maximum power point, which normally varies with illumination, radiation dose, temperature, and aging effects [19]. The output voltage, current, and power are also sensitive to above factors, and this effect should be taken into account in the design of PV arrays. Maximum power point technique (MPPT) is a method to control the terminal voltage of PV panels so that maximum power can be extracted. This is best illustrated in Figure 29.

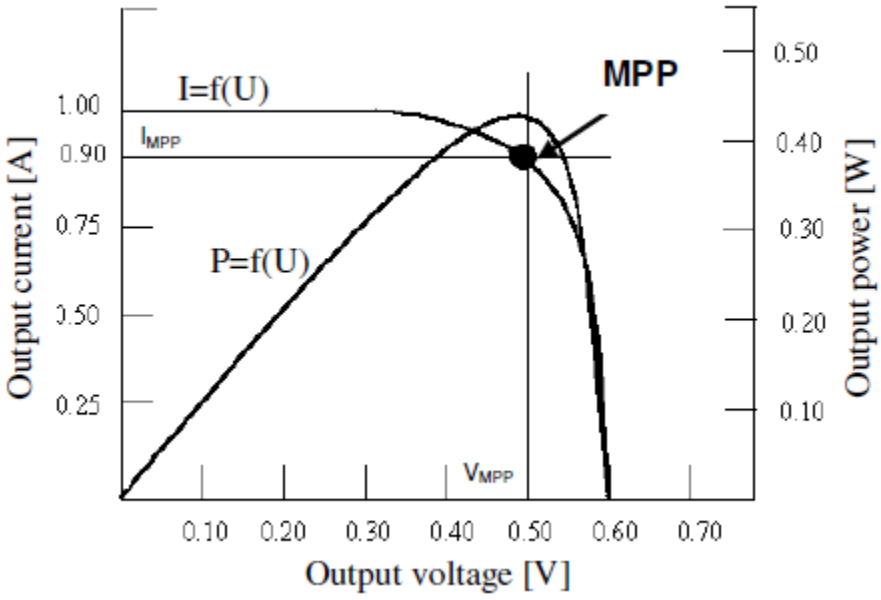

Figure 29: Typical I-V and P-V characteristics of a photovoltaic cell [19].

The open circuit voltage of the PV cell (V_{oc}) is the point of intersection of the curve with the horizontal axis and it changes very little with the change in solar radiation. If the temperature rises, it produces a decrease in the voltage. The point of intersection of the curve with the vertical axis is known as the short circuit current (I_{sc}), and it is directly proportional to solar radiation and is relatively insensitive to temperature variations. The PV module works like a constant current source for most parts of the I-V curve. The output power depends on the value of load. As the load increases, the operating point for the PV module moves to the right, and there is only one value of load which produces maximum power.

5.2 Modeling of PV cells

Modeling is a basic tool to capture behavior of real systems. In order to carry out the modeling of a PV cell, it is necessary to take into account the influence of various factors and also the characteristics given by producers of such devices. The mathematical models for PV cells are typically based upon theoretical equations that capture the operation of a PV cell and can be developed using equivalent circuit diagrams [19-25]. A second type of model for a PV cell is empirical in nature and it relies on different values extracted from I-V curve of PV arrays. Such models propose an analytical function that captures the behavior of a PV cell. Similar to the modeling of supercapacitors described in Chapter 4, the PV cell modeling is also carried out using MATLAB/Simulink environment or using other similar programs such as SPICE.

The equivalent circuit models are described in the following. The equivalent circuit of a general model which consists of a diode, a photo current, a parallel resistor expressing a leakage current, and a series resistance is shown in Figure 30a [20].

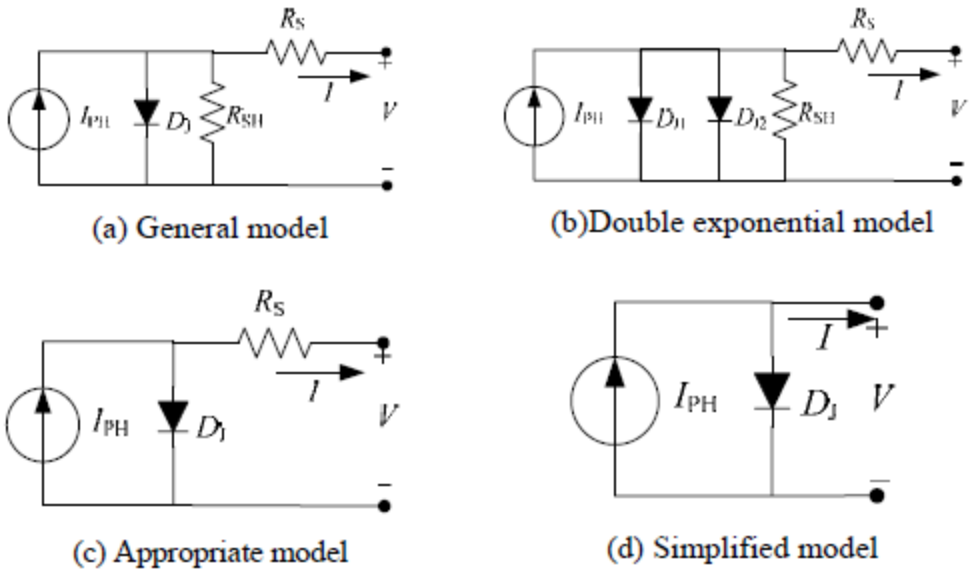

Figure 30: Different equivalent circuit models of a photovoltaic cell. R_S is a series resistance, R_{SH} is a shunt resistance, I_{PH} is light-generated photocurrent, and I_S is the cell saturation current.

A relatively more exact mathematical description of a solar cell known as the double exponential model is shown in Figure 30b. This model is derived from the physical behavior of the solar cell constructed from polycrystalline silicon. This model is made up of a current source, two diodes, a series resistance, and a parallel resistance. This model is not very frequently used for PV cells. The appropriate model of a PV cell is shown in Figure 30c. For an ideal PV cell, there is no series loss and no leakage to ground. The

equivalent model of such a cell is shown in Figure 30d. The voltage-current characteristic equations of a solar cell for different models are given as:

$$I=I_{PH}-I_S[exp(q(V+IR_S)/kT_CA)-1]-(V+IR_S)/R_{SH}\ \text{[General Model]} \quad (3)$$

$$I=I_{PH}-I_S[exp(q(V+IR_S)/kT_CA)-1]\ \text{[Appropriate Model]} \quad (4)$$

$$I=I_{PH}-I_S[exp(qV/kT_CA)-1]\ \text{[Simplified Model]} \quad (5)$$

Solar cells can also be connected in series-parallel configuration on a module to produce high power. This is known as a PV array which is just a group of several PV modules connected in series (N_s) and parallel (N_p) to generate required voltage and current. A general model, an appropriate model, and a simplified model of this type are shown in Figure 31.

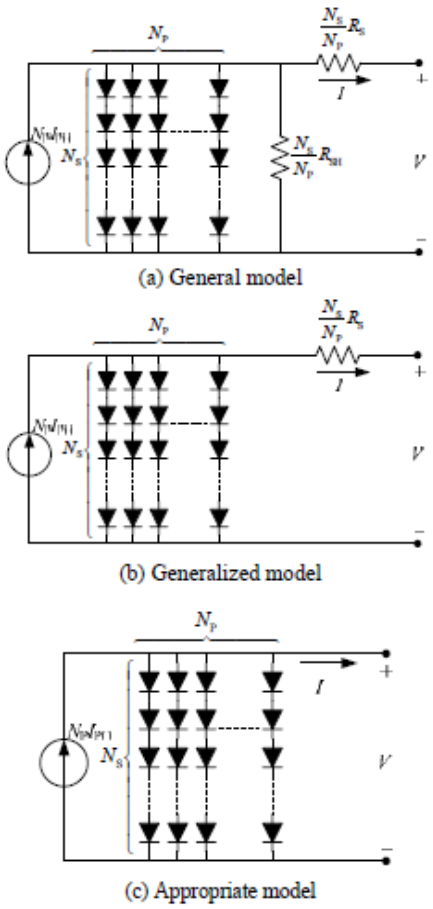

(a) General model

(b) Generalized model

(c) Appropriate model

Figure 31: Equivalent circuit models of generalized PV array.

Furthermore, it is possible to develop a generalized model of a PV module with moderate complexity which includes temperature independence of photocurrent source, the saturation current of diode and a series resistance. Such a model can be implemented in MATLAB/Simulink, and includes I-V and P-V non-linear characteristics of PV module. A subsystem implementation of such a model by Tsai et al. [20] is shown in Figure 32.

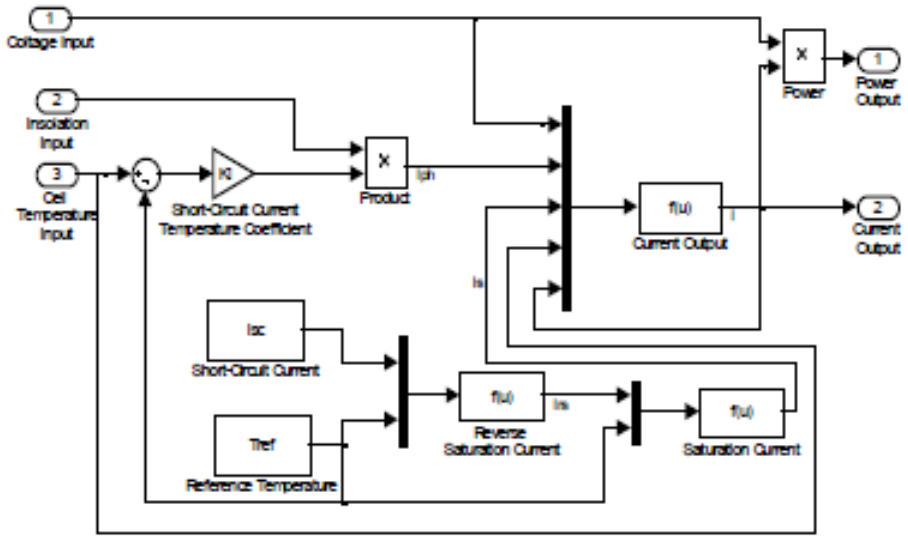

Figure 32: A subsystem implementation of a generalized PV module.

5.3 Output characteristics of different models

In order to measure the non-linear nature of I-V and P-V characteristics of a PV cell, one can vary the temperature as well as irradiance conditions (λ). The evolution of such characteristics with changing parameters is illustrated in Figure 33-34. The non-linear nature is apparent in these plots. Also, with the increase of working temperature, the

current increases, while the power decreases. On the other hand, with the increase of solar insolation, short-circuit current increases, and so does the maximum power output.

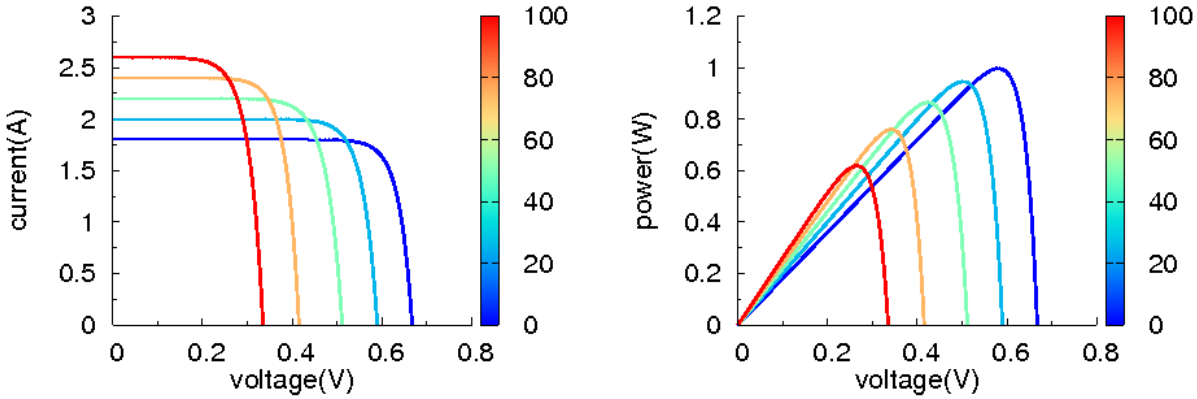

Figure 33: I-V and P-V characteristics of a PV module with different temperatures (T).

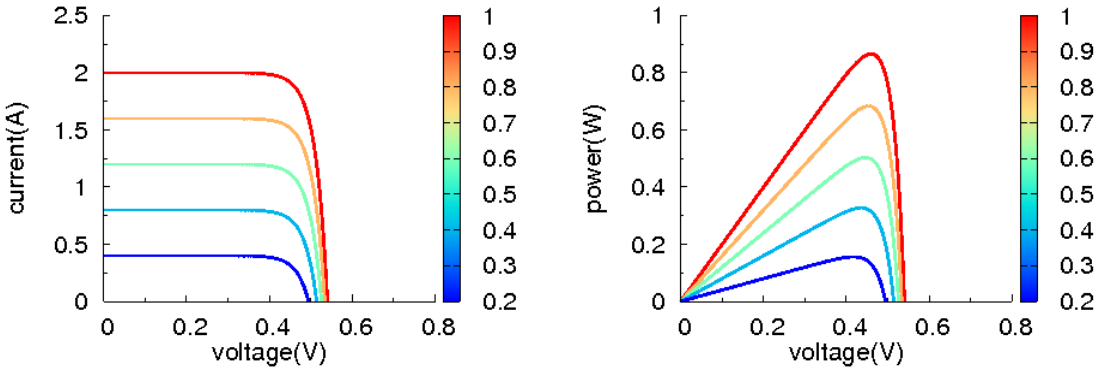

Figure 34: I-V and P-V characteristics of a PV module with different λ.

If experimental data are available, one can also create a model that can be optimized to match the experimental I-V characteristics of a PV cell.

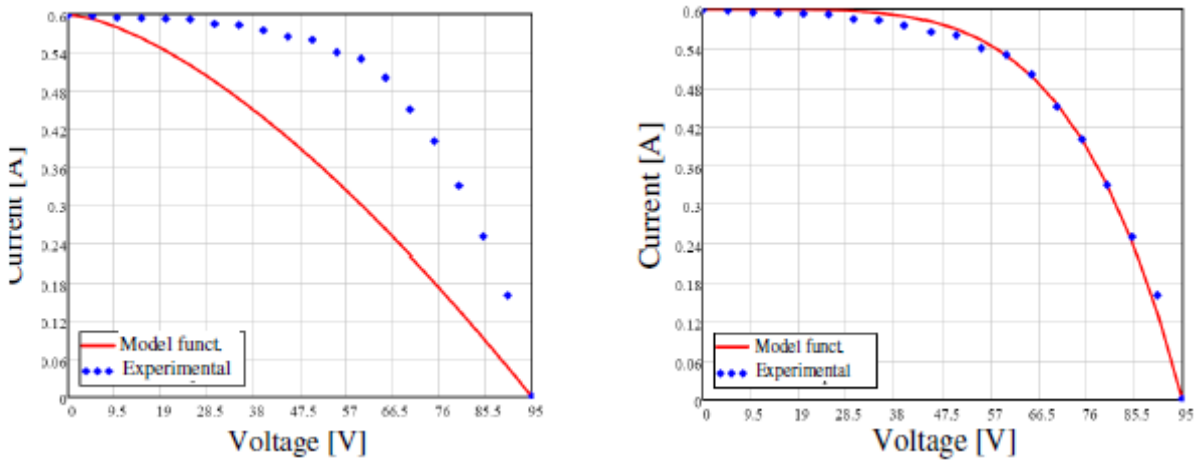

Figure 35: I-V characteristics of a PV module. (Left) before optimization, and (Right) after optimization.

Chapter 6: Outlook and conclusions

6.1 Introduction

Each of the devices discussed in this thesis face challenges for large-scale applications, both in terms of developing novel materials as well as new modeling and simulation methods. A wide variety of nanostructured materials, prepared either by deliberate design or by fortuitous reactions, is often advantageous for enhancing electronic, ionic, or oxygen transport properties in electrode materials for applications in various energy conversion and storage devices. Nanostructured approach allows one to tailor the material to suit the need, or to compensate for limitations inherent within one material. Such tailored and hybrid nanomaterials are at the forefront of latest research in designing highly efficient and cost effective energy conversion and storage systems. The availability of many simulation programs, particularly those programs that work with the MATLAB/Simulink environment, makes it easier to create sophisticated mathematical as well as electrical circuit models for many energy conversion and storage devices such as supercapacitors and photovoltaic cells. As an example, discussed below are some key challenges for future supercapacitor applications.

6.2 Challenges for future: Supercapacitors

One of the greatest challenges in the supercapacitor technology is the relatively high cost when compared to other energy devices. Thus future work in this technology is being devoted to carbon-based materials with high charge capacity in a cost effective way. It is expected that new generation of supercapacitors will replace batteries in certain applications, where high efficiency, high power, and high level of reliability is necessary.

Specifically, research and development work concerning hybrid supercapacitors, equivalent series resistance, electrolyte optimization, and self-discharge are likely to expand and enable huge advances in the performance of supercapacitors. The equivalent series resistance (ESR) of supercapacitors prevents these devices from achieving theoretical power densities. Therefore, lowering ESR of supercapacitors is likely going to be an important area of research. There are various ways of doing this which are being explored such as polishing the surface of current collectors, chemical bonding the electrode to the current collector, and using colloidal suspensions. The relationship between the pore size and ESR in electrode materials is also being explored.

A major area of research in supercapacitors is also the optimization of electrolyte because its resistance can significantly limit power density, while its ion concentration and operating voltage can limit the energy density of supercapacitors. Yet another key aspect to focus on in future will be to ameliorate the tendency of supercapacitors to self-discharge. The self-discharge occurs because of thermodynamic potential energy differences between charged and discharged supercapacitors. This problem is common to all energy conversion and storage devices such as batteries and simple capacitors, but the rate of self-discharge is higher for supercapacitors. If many of the aforementioned problems can be alleviated in future, supercapacitors have the potential of becoming realistic, widely available power solutions for a variety of applications. Supercapacitors are already being used in specialized applications and complement the strength of batteries in some cases. These applications may be in electric vehicle hybrid power systems, pulse power applications, and emergency power supplies, etc.

For modeling applications, among many programs discussed in this work, Simulink, SimPowerSystems, and PLECS have the advantage of direct access to MATLAB environment. Also, Simulink and OrCAD capture have large user bases, and may play a significant role in future modeling and simulation applications of energy conversion and storage devices.

References

1. P. Simon and Y. Gogotsi (2008). Materials for electrochemical capacitors. *Nature Materials*, doi: 10.1038/nmat2297.
2. L. Zhang and X. S. Zhao (2009). Carbon-based materials as supercapacitor electrodes. *Chem. Soc. Rev.* 38:2520-2531.
3. Nazar et al. (2001). Nanostructured materials for energy storage. *Int. J. of Inorganic Materials* 3:191-200.
4. Arico et al. (2005). Nanostructured materials for advanced energy conversion and storage devices. *Nature Materials* 4:366-377.
5. Bruce et al. (2008). Nanomaterials for rechargeable lithium batteries. *Angew. Chem. Int. Ed.* 47:2930-2946.
6. Y. Wang and G. Cao (2008). Developments in nanostructured cathode materials for high performance lithium ion batteries. *Adv. Materials* 20:2251-2269.
7. Guo et al. (2008). Nanostructured materials for electrochemical energy conversion and storage devices. *Adv. Materials* 20:2878-2887.
8. P. V. Kamat (2007). Meeting the clean energy demand: Nanostructure architectures for solar energy conversion. *J. Phys. Chem. C* 111:2834-2860.
9. Zhang et al. (2009). Zno nanostructures for dye-sensitized solar cells. *Adv. Materials* 21:4087-4108.
10. Wang et al. (2009). Supercapacitor devices based on graphene materials. *J. Phys. Chem. C* 113:13103-13107.

11. Danilla et al. (2011). Models and modelling the supercapacitors for a defined application. *Annals of the University of Craiova, Electrical Engineering Series* 35:200-205.

12. M. S. Halper and J. C. Ellenbogen (2006). Supercapacitors: A brief overview. *MITRE Nanosystems Group*. The MITRE Corporation, McLean, Virginia, USA.

13. G. Madabattula and S. K. Gupta (2012). Modeling of supercapacitor. *Excerpt from the proceeding of the 2012 COMSOL Conference in Bangalore.*

14. M. W. Verbrugge and P. Liu (2005). Microstructural analysis and mathematical modeling of electric double-layer supercapacitors. *J. Electrochem. Soc.* 152:D79-D87.

15. P. Johansson and B. Andersson (2008). Comparison of simulation programs for supercapacitor modeling. Master of Science Thesis. Department of Energy and Environment, Chalmers University of Technology.

16. Farcas et al. (2009). Modeling and simulation of supercapacitors. *15th International Symposium for Design and Technology of Electronics Packages.*

17. J. Qu and L. Liang (2012). Modeling and simulation for supercapacitor braking energy recovery process of micro EV. *Adv. Mat. Res.* 383:7390-7395.

18. Martynyuk et al. (2010). Investigation of the supercapacitor mathematical model by means of LTspiceIV.

19. Petreus et al. (2008). Modelling and simulation of photovoltaic cells. *Acta Technica Napocensis* 49:42-47.

20. Tsai et al. (2008). Development of generalized photovoltaic model using MATLAB/Simulink. *Proceedings of the World Congress on Engineering and Computer Science.* San Francisco, USA.
21. J. S. Kumari and C. S. Babu (2012). Mathematical modeling and simulation of photovoltaic cell using MATLAB-Simulink environment. *Int. J. Comp. Elec. Eng*. 2:26-34.
22. Salmi et al. (2012). MATLAB/Simulink based modeling of solar photovoltaic cell. *Int. J. Renew. Energy Res.* 2:213-218.
23. N. Pandiarajan and R. Muthu (2011). Mathematical modeling of photovoltaic module with Simulink. *Int. Conf. Elec. Energy Sys.* 258-263.
24. S. S. Mohammed (2011). Modeling and simulation of photovoltaic module using MATLAB/Simulink. *Int. J. Chem. Environ. Eng.* 2:350-355.
25. G. Venkateswarlu and P. Raju (2012). Simulink based model of photovoltaic cell. *Int. J. Mod. Eng. Res.* 2:2668-2671.

Appendices

Provided below is the GNUPLOT script to reproduce I-V and P-V characteristics of a photovoltaic cell presented in Figure 33.

```
set term post eps enh color solid size 6,4 "Helvetica" 38

set output "temp_I-V.eps"

set key t r spacing 1.2 samplen 4.0 invert nobox inside

set xzeroaxis lt 0 lw 2.5

#set yzeroaxis lt -1 lw 1.5

set ytics 0,0.5,3     font "Helvetica,38"  nomirror

set xtics 0,0.2,0.8     font "Helvetica,38"  nomirror

set xrange[0:0.8]

set yrange[0:3]

set mytics 2

set mxtics 2

set border 3

set tics scale 1.5
```

```
set xlabel 'voltage(V)'          font "Helvetica,38" offset
0,0.5

set ylabel 'current(A)'  font "Helvetica,38"  offset 1.0

set palette rgbformulae 22,13,10

set style line 1 lt 1 lc palette fraction 0.0  lw 8 pt 7 ps
2

set style line 2 lt 1 lc palette fraction 0.25 lw 8 pt 7 ps
2

set style line 3 lt 1 lc palette fraction 0.50 lw 8 pt 7 ps
2

set style line 4 lt 1 lc palette fraction 0.75 lw 8 pt 7 ps
2

set style line 5 lt 1 lc palette fraction 1.0  lw 8 pt 7 ps
2

set cbrange[0:100]

A1=1.8

A2=2.0

A3=2.2

A4=2.4
```

```
A5=2.6

B1=1.E-10

B2=1.E-8

B3=0.5E-6

B4=1E-6

B5=0.5E-4

k=1.38E-23

q=1.6E-19

A=1.2

T1=273

T2=298

T3=323

T4=348

T5=373

C=(q)/(k*A)

I1(x) =(A1-B1*(exp((C/T1)*x)-1))

I2(x) =(A2-B2*(exp((C/T2)*x)-1))

I3(x) =(A3-B3*(exp((C/T3)*x)-1))
```

```
I4(x) =(A4-B4*(exp((C/T4)*x)-1))

I5(x) =(A5-B5*(exp((C/T5)*x)-1))

 plot I1(x) w l ls 1 notitle,\

     I2(x) w l ls 2 notitle,\

     I3(x) w l ls 3 notitle,\

     I4(x) w l ls 4 notitle,\

     I5(x) w l ls 5 notitle

set output "temp_P-V.eps"

set ytics 0,0.2,1.2     font "Helvetica,38"  nomirror

set yrange[0:1.2]

set ylabel 'power(W)'  font "Helvetica,38"  offset 1.0

plot x*I1(x) w l ls 1 notitle,\

     x*I2(x) w l ls 2 notitle,\

     x*I3(x) w l ls 3 notitle,\

     x*I4(x) w l ls 4 notitle,\

     x*I5(x) w l ls 5 notitle
```

Provided below is the GNUPLOT script to reproduce I-V and P-V characteristics of a photovoltaic cell presented in Figure 34.

```
set encoding iso_8859_1

set term post eps enh color solid size 6,4 "Helvetica" 38

set output "lambda_I-V.eps"

set key t r spacing 1.2 samplen 4.0 invert nobox inside

set xzeroaxis lt 0 lw 2.5

#set yzeroaxis lt -1 lw 1.5

set ytics 0,0.5,2.5     font "Helvetica,38"  nomirror

set xtics 0,0.2,0.8     font "Helvetica,38"  nomirror

set xrange[0:0.8]

set yrange[0:2.5]

set mytics 2

set mxtics 2

set border 3

set tics scale 1.5
```

```
set xlabel 'voltage(V)'          font "Helvetica,38" offset
0,0.5

set ylabel 'current(A)'  font "Helvetica,38"  offset 1.0

set palette rgbformulae 22,13,10

set style line 1 lt 1 lc palette fraction 0.0  lw 8 pt 7 ps
2

set style line 2 lt 1 lc palette fraction 0.25 lw 8 pt 7 ps
2

set style line 3 lt 1 lc palette fraction 0.50 lw 8 pt 7 ps
2

set style line 4 lt 1 lc palette fraction 0.75 lw 8 pt 7 ps
2

set style line 5 lt 1 lc palette fraction 1.0  lw 8 pt 7 ps
2

set cbrange[0.2:1.0]

A1=1.8

A2=2.0

A3=2.2

A4=2.4
```

```
A5=2.6

B1=1.E-10

B2=1.E-8

B3=0.5E-6

B4=1E-6

B5=0.5E-4

k=1.38E-23

q=1.6E-19

A=1.2

T1=273

T2=298

T3=323

T4=348

T5=373

C=(q)/(k*A)

I1(x) =(A2*1.0-B2*(exp((C/T1)*x)-1))

I2(x) =(A2*0.8-B2*(exp((C/T1)*x)-1))

I3(x) =(A2*0.6-B2*(exp((C/T1)*x)-1))
```

```
I4(x) =(A2*0.4-B2*(exp((C/T1)*x)-1))

I5(x) =(A2*0.2-B2*(exp((C/T1)*x)-1))

 plot I1(x) w l ls 5 notitle,\

     I2(x) w l ls 4 notitle,\

     I3(x) w l ls 3 notitle,\

     I4(x) w l ls 2 notitle,\

     I5(x) w l ls 1 notitle

set output "lambda_P-V.eps"

set ytics 0,0.2,1.     font "Helvetica,38"  nomirror

set yrange[0:1.]

set ylabel 'power(W)'  font "Helvetica,38"  offset 1.0

plot x*I1(x) w l ls 5 notitle,\

     x*I2(x) w l ls 4 notitle,\

     x*I3(x) w l ls 3 notitle,\

     x*I4(x) w l ls 2 notitle,\

     x*I5(x) w l ls 1 notitle
```